Science of the Total Environment 943 (2024) 173670

Contents lists available at ScienceDirect

Science of the Total Environment

journal homepage: www.elsevier.com/locate/scitotenv

Functional and compositional responses of stream microphytobenthic communities to multiple stressors increase and release in a mesocosm experiment

Ntambwe Albert Serge Mayombo [a,*], Andrea M. Burfeid-Castellanos [a], Anna-Maria Vermiert [b], Iris Madge Pimentel [c], Philipp M. Rehsen [c], Mimoza Dani [a], Christina Jasinski [a], Marzena Agata Spyra [a], Michael Kloster [a], Danijela Vidaković [a,d], Dominik Buchner [c], Bánk Beszteri [a]

[a] Phycology, Faculty of Biology, University of Duisburg-Essen, Essen, Germany
[b] Department of Animal Ecology, Evolution and Biodiversity, Faculty of Biology and Biotechnology, Ruhr University Bochum, Bochum, Germany
[c] Aquatic Ecosystem Research, Faculty of Biology, University of Duisburg-Essen, Essen, Germany
[d] Institute of Chemistry, Technology and Metallurgy, National Institute of the Republic of Serbia, University of Belgrade, Belgrade, Serbia

HIGHLIGHTS

- Multiple stressors (e.g. reduction in flow velocity, increase in salinity and temperature) threaten urban streams.
- Diatom and microalgae communities and their photosynthetic biomass were examined in a stream mesocosm experiment.
- Reduced flow velocity and increased temperature had a greater effect on microphytobenthic communities and biomass.
- Possible memory effect of salinity on eukaryotic microalgae assemblages.
- Following stressor treatment, recovery resulted in a convergence of community composition with priority effects.

GRAPHICAL ABSTRACT

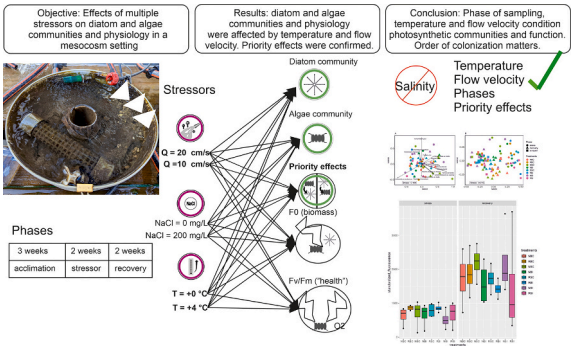

ARTICLE INFO

Keywords:
Chlorophyll fluorescence
Diatoms
Microalgae
ExStream system
Digital microscopy
18S-V9 amplicon sequencing

ABSTRACT

Field observations form the basis of the majority of studies on microphytobenthic algal communities in freshwater ecosystems. Controlled mesocosm experiments data are comparatively uncommon. The few experimental mesocosm studies that have been conducted provide valuable insights into how multiple stressors affect the community structures and photosynthesis-related traits of benthic microalgae. The recovery process after the stressors have subsided, however, has received less attention in mesocosm studies. To close this gap, here we present the results of a riparian mesocosm experiment designed to investigate the effects of reduced flow velocity, increased salinity and increased temperature on microphytobenthic communities. We used a full factorial design with a semi-randomised distribution of treatments consisting of two levels of each stressor ($2 \times 2 \times 2$ treatments), with eight replicates making a total of 64 circular mesocosms, allowing a nuanced examination of their individual and combined influences. We aimed to elucidate the responses of microalgae communities seeded from stream water to the applied environmental stressors. Our results showed significant effects of

* Corresponding author.
E-mail address: ntambwe.mayombo@uni-due.de (N.A.S. Mayombo).

https://doi.org/10.1016/j.scitotenv.2024.173670
Received 6 December 2023; Received in revised form 17 May 2024; Accepted 29 May 2024
Available online 4 June 2024

reduced flow velocity and increased temperature on microphytobenthic communities. Recovery after stressor treatment led to a convergence in community composition, with priority effects (hypothesized to reflect competition for substrate between resident and newly arriving immigrant taxa) slowing down community shifts and biomass increase. Our study contributes to the growing body of literature on the ecological dynamics of microphytobenthos and emphasises the importance of rigorous experiments to validate hypotheses. These results encourage further investigation into the nuanced interactions between microphytobenthos and their environment and shed light on the complexity of ecological responses in benthic systems.

1. Introduction

Freshwater ecosystems are dynamic and rich in biodiversity. They are closely linked to all environmental ecosystems and are therefore vulnerable to anthropogenic activities in the catchment areas. These vital habitats face numerous challenges due to multiple anthropogenic stressors. In this context, any disturbance factor that causes environmental variables, individuals, populations, communities, or ecosystem functions to exceed the range of normal variation relative to undisturbed reference conditions is referred to as an anthropogenic stressor (Vos et al., 2023). Freshwater salinization is one of the most pressing stressors (Cañedo-Argüelles et al., 2013), and in addition to measuring and monitoring the ion contents of water bodies, it is important to know how salinization impacts ecosystems and their communities. Inland water salinization can occur naturally, as observed in permanent and ephemeral saline lakes where evaporation typically exceeds annual rainfall (Stenger-Kovács et al., 2023). This is referred to as primary salinization. Yet, secondary salinization of rivers and streams, resulting from human activities like agriculture, water withdrawal, road salt application, mining effluents, sea level rise, and climate change, can significantly alter freshwater communities (Cañedo-Argüelles et al., 2013; Cunillera-Montcusí et al., 2022). This human-induced salinization not only affects the structure and function of aquatic communities but also impacts the benefits, known as ecosystem services, that we derive from these ecosystems (Cañedo-Argüelles et al., 2013; Cunillera-Montcusí et al., 2022; Kelly et al., 2023).

In addition, global warming - a hallmark of anthropogenic climate change - adds thermal stress that has cascading effects on species distributions, metabolic rates, and interspecific interactions (Striebel et al., 2016; Lengyel et al., 2023b). There are several direct (e.g. changes in individual growth rates, photosynthetic efficiency, and cellular biochemistry) and indirect effects (e.g. via changes in nutrient availability, concentration of dissolved gases, pH, and water column stability) of water temperature on aquatic ecosystems (Bondar-Kunze et al., 2021; Siegel et al., 2023). Furthermore, changes in flow rates caused by factors such as erratic precipitation patterns leading to flooding or drought, dam constructions, diversions, and numerous other forms of infrastructure, resulting in the reduction or elimination of flooding and other ecologically important aspects of flow regimes, can affect habitat structures and nutrient availability (Tonkin et al., 2018; Bondar-Kunze et al., 2021). These anthropogenic stressors can have profound and often unpredictable impacts on freshwater ecosystems (Piggott et al., 2015).

Microphytobenthic communities form an essential component of freshwater ecosystems. They are also known as periphyton, often dominated by diatoms (Bacillariophyta). Periphyton form the biofilm that inhabits the benthic interface of water bodies and contributes significantly to primary production through photosynthesis (Lengyel et al., 2023b). Their role extends beyond primary production to nutrient cycling and sediment stabilisation, and they form the basis of food webs (B-Béres et al., 2023; Lengyel et al., 2023a). Given their central role in ecosystem dynamics, it is crucial to decipher how they respond to the anthropogenic stressors mentioned above for both nature conservation and complying with the European Commission's Water Framework Directive (European Commission, 2000).

Understanding the responses of microphytobenthos (MPB) assemblages to multiple stressors is not only a scientific endeavour but an urgent ecological imperative. It is well established that the photosynthetic activity (Silva, 2000), and community structure of diatoms (Dixit et al., 1999; Virtanen and Soininen, 2012; Schröder et al., 2015; Heikkinen et al., 2022) are both affected by prolonged exposure to salt. Yet, characterising salinity's specific influence on species composition and freshwater ecosystem functioning remains challenging (Castillo et al., 2018; Stenger-Kovács et al., 2023). In addition, increasing water temperature and reduced water flow velocity are both important factors that influence periphyton, though water chemistry is perceived to play a more crucial role in driving their community composition (Hering et al., 2006; Marcel et al., 2017). The relatively low number of studies testing the effects of multiple stressors on freshwater microphytobenthos, compared to the diversity of stressors to be selected, makes it difficult to distinguish clear general patterns when it comes to their interactive effects. If a stressor is interactive it interacts positively (in the same direction, synergism) or negatively (in opposite direction, antagonism) with a second or third stressor. Very few studies have explored the interactions between stressors on one hand and the dynamics of recolonization on the other (Piggott et al., 2015).

Diatoms have a well-established global reputation in biomonitoring studies owing to their exceptional bioindication capabilities (Lobo et al., 2016). They are particularly valuable for evaluating ecosystem recovery following environmental disturbances, as evidenced in lotic ecosystem research (Steinman and McIntire, 1990; Brown and Manoylov, 2023). Notably, significant shifts in diatom communities have been well-documented in correlation with eutrophication in streams and rivers. Efforts to mitigate nutrient inputs, aimed at restoring these ecosystems to their original state have yielded ambiguous outcomes and often failed to achieve a full return to the pre-disturbance conditions (Brown and Manoylov, 2023). According to this study, ecosystem recovery is a complex process that involves more than just reversing the pathway of degradation. It may take several decades to complete or, in the case of some streams and rivers, may not occur at all (Brown and Manoylov, 2023). The recently introduced Asymmetric Response Concept (ARC, Vos et al., 2023) highlights the differences between degradation and recovery pathways of biological communities in terms of the relative contribution of processes that determine community assembly, such as abiotic tolerances, biotic interactions and dispersal. These processes can vary in speed and outcome, potentially leading to new ecosystem states or even failure. While some studies have suggested that diatom communities may require several decades to recover fully, others have reported signs of recolonization in a matter of weeks. However, these quick recolonization observations have typically relied on ecological indices rather than comprehensive community composition assessments (Peterson et al., 1990; Steinman and McIntire, 1990; Lacoursière et al., 2011; Duong et al., 2012).

Most freshwater microphytobenthic community studies are based on field observations of diatom assemblages, while data from controlled mesocosm experimental settings are relatively scarce. The few experimental studies that have been conducted have provided valuable insights into the impact of single stressors, such as light availability, flow velocity, sediment, nutrients, temperature, and salinity, as well as their combinations, on the community structures and functional traits of benthic diatoms (Piggott et al., 2015; Bondar-Kunze et al., 2016; Nuy et al., 2018; Costello et al., 2018; Salis et al., 2019; Bondar-Kunze et al., 2021; Frost et al., 2023). However, the recovery process after the

alleviation of these stressors is less studied, we could not find any prior mesocosm studies that have examined the recovery of microphytobenthos communities following the alleviation of stressors.

In the present study, we attempt to address the question of how the microphytobenthic algal communities change, develop, and potentially restructure in the face of anthropogenic pressures and changing climatic conditions, using a highly replicated streamside mesocosm experiment. Our primary objective is to contribute valuable insights to the management and conservation of freshwater ecosystems by conducting a comprehensive investigation into the multifaceted impacts of various stressors on microphytobenthos communities. Our study is based on two specific hypotheses: First, we hypothesize that stressors lead to a shift in community composition toward lower diversity and increased dominance of disturbance-tolerant taxa, while having a relatively limited impact on photosynthetic biomass. Second, we expect that priority effects, i.e. occupancy of physical and niche space by a resident community, will initially hinder recolonization by immigrant species when stressor load is alleviated. This initial asymmetry in recovery is expected to be observable over weeks such that the microphytobenthos community structure in stressed mesocosms will remain different from that of the unstressed control.

2. Materials and methods

2.1. Study site and experimental design

The Emscher/Boye catchment, located in the highly urbanised Ruhr Metropolitan Region of Northern Germany, has a long history of severe anthropogenic impacts. For centuries, the densely populated Ruhr Metropolitan Area used this river system as an open sewer to help release untreated wastewater from domestic, industrial coal mining operations and agricultural surface runoff activities. Since 1990s, the Emschergenossenschaft, a local water management authority, initiated restoration projects at various parts of the catchment to stop and revert the negative impacts of anthropogenic disturbances in this river network (Winking et al., 2014, 2016). However, in the context of these habitat restoration efforts, the critical aspect of ecosystem dynamics of microphytobenthic communities after restoration of the Emscher/Boye catchment remains unexplored. The background physical and chemical measurements taken bi-weekly in the river during the experiment are listed in Table 1.

We used a streamside mesocosm experimental setup (ExStream System, Piggott et al., 2015) consisting of 64 circular mesocosms to decipher the functional and compositional responses of stream microphytobenthos communities to multiple stressors. The experiment was conducted in the Boye River (51.5533°N, 6.9485°E). In the experimental system, untreated water was redirected from the Boye River to flow through circular mesocosms (Fig. 1A/C). Water was pumped from the river using two pumps (Pedrollo NGAm 1A-pro) into two settling tanks placed on top of the scaffolding structure (Fig. 1B). The water entering the system was divided into four spatial blocks (B1-B4, each having 16 circular mesocosm channels) via a distributor and then passed through a 203 L sediment trap in which the flow velocity was reduced so that fine suspended material could settle to the bottom of the tank. The water was then passed into a second sediment trap, where further sedimentation could take place. The water then entered the header tank (Fig. 1B), which supplied the mesocosms (outer diameter: 25 cm, central outflow: 6 cm, volume 3.5 L, area: 450 cm^2; Microwave Ring Moulds, Interworld, Auckland, New Zealand, Fig. 1C). Using a shut-off valve, the inflow in the mesocosms was calibrated twice a day to roughly 2.1 L/min. Excess water was discharged via an overflow at the top of each collection tank into the system's outfall, where it was filtered through a retention basin and finally discharged back into the Boye River downstream of the system's intake.

The experiment ran for 48 days from 4th March to 21st April 2022, starting with 20 days (March 4 – March 24) of colonization and acclimation. After that, stressors were introduced into the mesocosms for 14 days (March 24 – April 7, the stressor phase), and then a 14-day recovery period (April 7 – April 21, the recovery phase) with no applied stressors. We employed a full factorial design (2 × 2 × 2) with a random distribution of flow velocity and salinity treatments, and a block-wise distribution of temperature treatments (Table 2), consisting of two levels of each stressor, with eight replicates. However, due to an error, a salinization treatment was incorrectly assigned to a different mesocosm, resulting in variations in the number of replicates for different treatments, such as nine replicates for the treatments reduced flow velocity combined with warming (C08, F + T, see Table 2) and salinization combined with warming (C07, S + T, see Table 2). During the 14-day stressor phase, we aimed to expose the stressed mesocosms to increased temperature + 4 °C (± 0.2 °C) vs ambient (control) (Fig. 2A, also see Fig. S1A), increased salinity (+ 200 mg/L chloride) vs background (Fig. 2B, also see Fig. S1B, C), and reduced flow velocity (~10 cm/s) vs normal (~20 cm/s) (Table 2).

To reduce flow velocity, the inflow jet was removed without affecting water volume. This resulted in two flow velocities: normal flow velocity (14.25 ± 7.59 cm/s, n = 4) with the inflow jet and reduced flow velocity (3.50 ± 3.32 cm/s, n = 4) without it. This significantly reduces flow velocity as would be caused by human activities such as water abstraction, morphological changes, etc. To induce salt stress, a concentrated NaCl solution (> 350 mg/L) was prepared by dissolving salt tablets (Claramat, >99.9 % NaCl) in stream water. This solution was fed into an irrigation pipe via dosage pumps (GHL Doser 2.1, at a rate of approx. 714 mL/min). The irrigation pipe was additionally supplied with filtered stream water (mesh size 100 μm) and pressure-compensated drippers released the water from the irrigation pipe to the salt-treated mesocosms at a rate of 4 L/h. Initially, a motor-driven agitator was used for salt dissolution, but it caused undissolved salt tablets to block the suction hoses of the dosing pumps. Therefore, the agitator was replaced with a submersible pump (Gardena, 9000Dirt) for mixing on the following day, delaying the start of salinization by one day. Heating was achieved by warming water in collection tanks, and a mixing module allowed quick temperature adjustments while minimizing high-temperature exposure to organisms. Temperature (Fig. 2A) was recorded every 5 min in two randomly selected mesocosms per block (HOBO Pendant MX Temp/Light) and electrical conductivity (EC,

Table 1
Background physical and chemical parameters measured bi-weekly during the experiment. Conductivity, pH, dissolved oxygen, water temperature and water level were measured in situ, while ortho-phosphate, total phosphate, ammonia, nitrite, nitrate, total nitrogen, chloride, sulfate and dissolved organic carbon (DOC) are lab measurements.

Date	25/02/2022	11/03/2022	25/03/2022	07/04/2022	21/04/2022
pH	8.18	8.13	NA	8.01	8.21
Conductivity (μS/cm)	594	793	NA	600	796
Dissolved oxygen (mg/L)	7.3	10.7	NA	14.4	14.2
Water temperature (°C)	5.6	5.1	NA	7.8	10.6
Water level (cm)	56	36.7	NA	50	31.5
Ortho-phosphate (mg/L)	0.023	0	0.012	0.028	0.011
Total Phosphate (mg/L)	0.024	0.020	0.033	0.049	0.026
Ammonia (mg/L)	0.103	0.191	0.15	0.127	0.076
Nitrite (mg/L)	0.032	0.074	0.081	0.068	0.052
Nitrate (mg/L)	17.303	7.273	7.823	11.901	6.141
Total Nitrogen (mg/L)	3.998	1.813	1.908	2.808	1.462
Chloride (mg/L)	30.673	25	37	28	37
Sulfate (mg/L)	96	107	159	105	160
DOC (mg/L)	NA	17.24	16.69	21.21	16.4

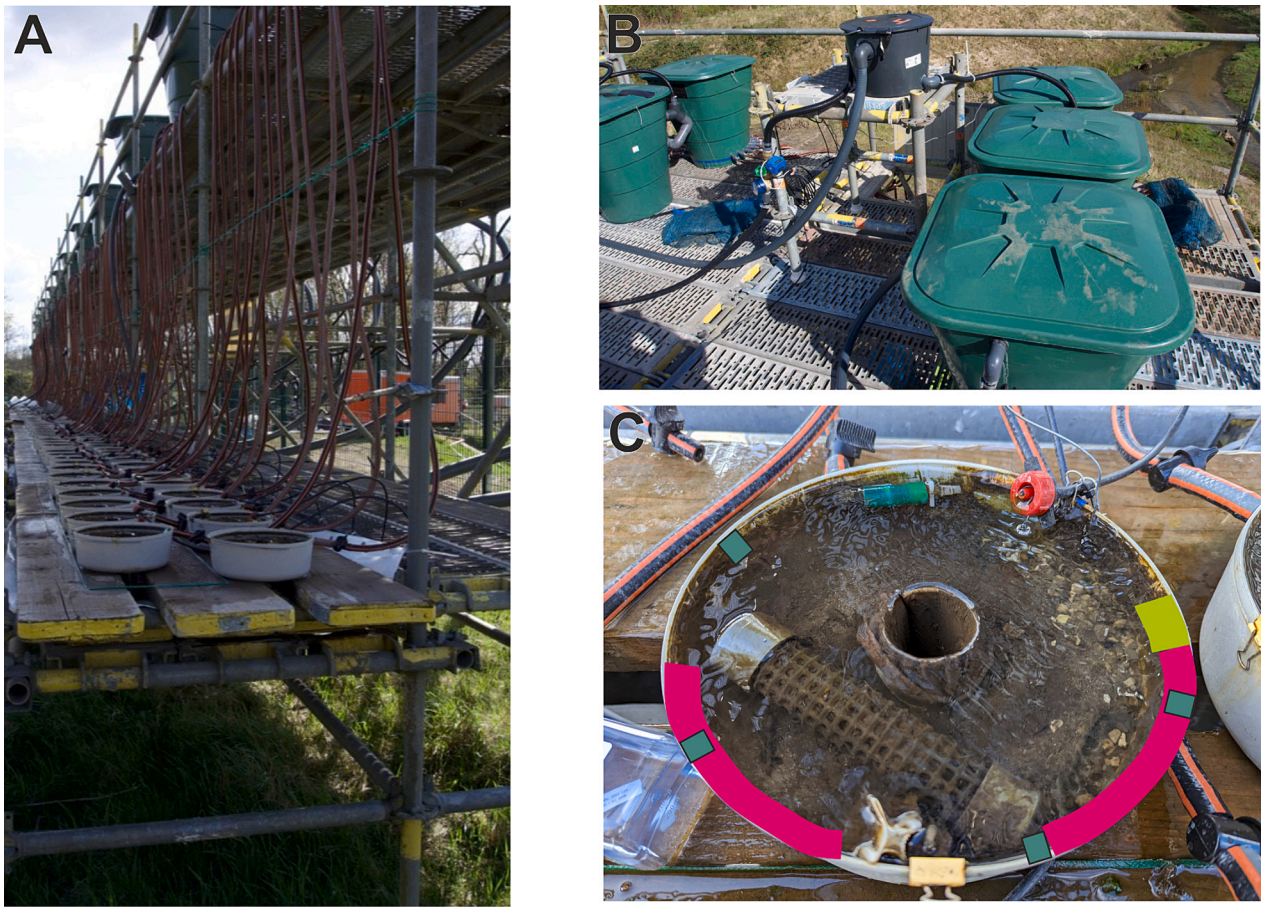

Fig. 1. ExStream experimental setup show A) circular mesocosms; B) header tanks (green) and small heating bucket (black); C) Inside the circular mesocosm channel showing the dripping line for salt treatment, the area scraped for biofilm recovery in light green, area scraped for different biofilm samples analysed in this study red, and areas where MINI-PAM II measurement were done (dark green).

Table 2
Glossary and treatment distribution. In bold "problematic" channels explained in the experimental design.

Code	Short	Flow	Salinity	Temperature	Phase	Channels
C	Control	Normal	Background	Control	Stressor	C21, C23, C35, C43
					Recovery	C18, C19, C37, C42,
T	Increased temperature	Normal	Background	Increased	Stressor	C05, C62, C63
					Recovery	C04, C09, C52, C54
S	Increased salinity	Normal	Salt-treatment	Control	Stressor	C25, C26, C38, C47
					Recovery	C27, C31, C36, C44
F	Reduced flow	Reduced	Background	Control	Stressor	C28, C30, C33, C39
					Recovery	C22, C29, C34, C46
S + T	Salt + Temperature	Normal	Salt treatment	Increased	Stressor	**C07**, C13, C15, C49, C50
					Recovery	C14, C16, C53, C60
F + T	Flow + Temperature	Reduced	Background	Increased	Stressor	C06, **C08**, C10, C56, C59
					Recovery	C01, C12, C55, C57
F + S	Flow + Salinity	Reduced	Salt-treatment	Control	Stressor	C17, C24, C40, C48
					Recovery	C20, C32, C41, C46
F + S + T	Flow + Salinity + Temperature	Reduced	Salt-treatment	Increased	Stressor	C11, C61, C62
					Recovery	C02, C03, C58, C64

a proxy for salinity, Fig. 2B) was measured daily in all mesocosms using a WTW Cond 315i probe. If significant flow velocity reductions were observed during discharge calibration, an EC measurement was performed before making discharge adjustments.

The warming treatment was interrupted for three and a half days between stressor day 6 and the evening of stressor day 9 because a defective pump had to be replaced. Both warming and salt treatment were stopped for stressor day 13 and the night of stressor day 14 because heavy rainfall resulted in high sediment loads in stream water. This made maintaining the system challenging and the risk of blockages in the filter system and tubing leading to the mesocosms was too high to keep the stressors running. While the stressor treatments were effective (9 days of warming and 11 days of salinization), the average increase in water temperature between warmed and surrounding mesocosms was 3.45 °C (treatment means ± SD: ambient temperature = 8.71 ± 0.06 °C, warming = 12.16 ± 0.08 °C, n = 4). This is close to +3.26 °C of the projected temperature increase under SSP5–8.5 scenario in March (2080–2090). The average conductivity increase between background

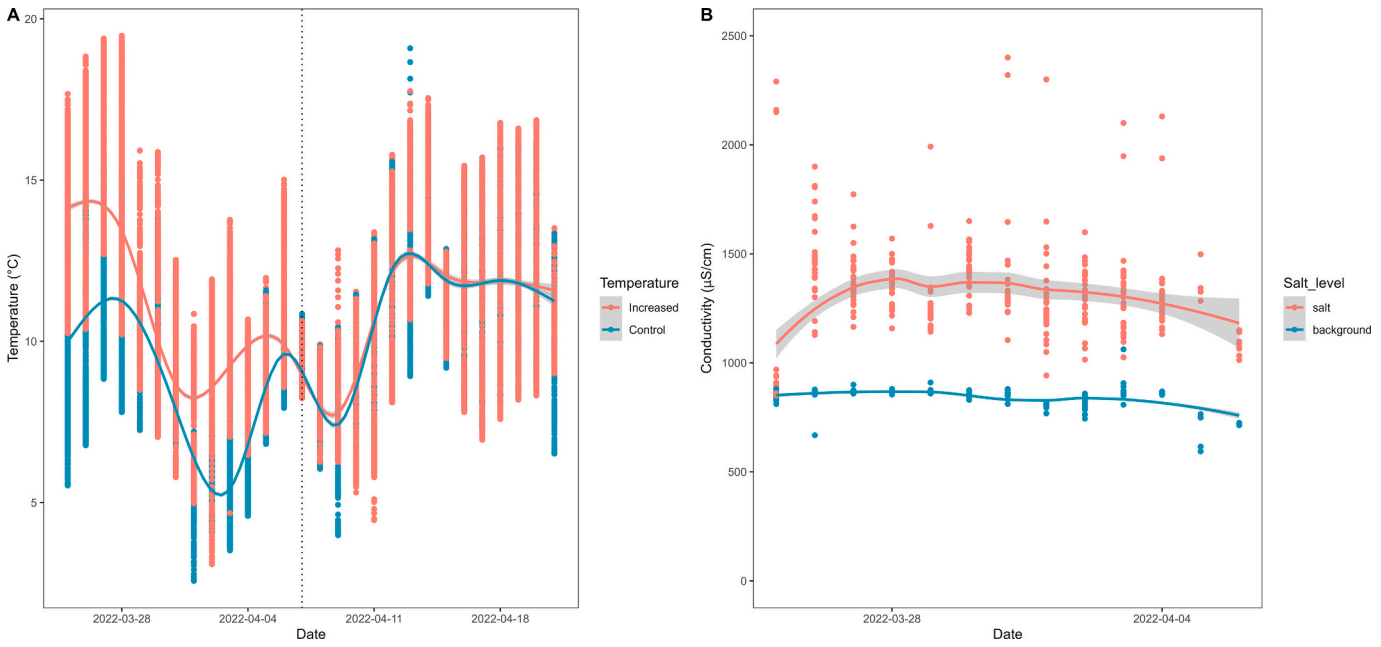

Fig. 2. Plot showing time-series dataset of A) temperature (stressor and recovery phases) and B) conductivity (only stressor phase) treatments applied in this study. The vertical dotted line separates the stressor application (left) from the stressor alleviation (right) phase.

salinity and elevated salinity was 0.529 mS/cm (treatment mean ± SD: $EC_{ambient}$ = 0.842 ± 0.006 mS/cm, EC_{salt} = 1.343 ± 0.151 mS/cm), corresponding to 154.1 mg/L added chloride (see Fig. S1). For the above calculations, short-term salinity peaks due to flow reductions have been removed. Our goal was to slightly exceed the maximum observed conductivity in the Boye catchment, which averages 1413 µS/cm at Nattbach, our experiment site. At the end of the 14-day stressor phase, half of the mesocosms from each treatment and their combinations were sampled. The remaining half were allowed to recover for 14 days. During this time, the inflow jet was reattached in all mesocosms with a reduced flow velocity treatment and the heating and salinization treatments were discontinued. The experiment ended with sampling of the recovery mesocosms on April 21, 2022.

Chlorophyll fluorescence following dark adaptation of microphytobenthic biofilm was monitored every 3 to 4 days during the stressor and recovery phase using a MINI-PAM II fluorometer (Heinz Walz GmbH, Effeltrich, Germany) to accurately quantify photosynthetic health (Y(II) or Fv/Fm) and biomass (F_0 or Fm) in situ throughout the experiment (Schreiber, 1986; Honeywill et al., 2002). The maximum quantum yield of photosystem II, also known as maximum efficiency of light utilization (Y(II) or Fv/Fm) is an indicator of health, while the minimum (F_0) and the maximum (Fm) fluorescence yield are indicators of biomass (Honeywill et al., 2002). Four positions along the internal wall of the mesocosm channel were selected and measured for photosynthetic activity (Fig. 1C, dark green points). Saturation pulse measurements were made in the evenings, always at least 30 min after dusk, so that dark-adapted biofilms were measured. Biofilm samples were collected from half of the mesocosm channels (32) at the end of the stressor phase. The remaining half of the mesocosm channels (32) were allowed to recover after the release of the stressors and were sampled at the end of the recovery phase. In addition, the biofilm in the remaining channels was completely scraped over an area of approximately 2 cm × 2 cm at the end of the stressor application phase, to monitor de novo recolonization using MINI-PAM II.

During sampling (end of stressor and recovery phases), biofilm was scraped from the internal walls of the mesocosms using plastic razor blades. Two samples were collected; one was taken over an area of approximately 5 × 20 cm^2 of mesocosms into 30 mL falcons (Fig. 1C pink-red), and fixed with 20 mL 96 % ethanol for digital microscopy for detailed diatom community observations (Burfeid-Castellanos et al., 2022) and 18S—V9 amplicon sequencing to reveal the broader microphytobenthic community dynamics (Amaral-Zettler et al., 2009). Another sample was collected over an area of about 1 × 1 cm^2 and preserved in 1.5 mL Eppendorf tubes with 96 % ethanol for lab chlorophyll extraction and measurements using a Tecan microplate reader (Mandalakis et al., 2017). Separate samples of biofilms were collected at the scraped surface area (2 × 2 cm) for 18S—V9 amplicon sequencing.

2.2. *Lab sample preparation for chlorophyll extraction, digital microscopy and 18S—V9 amplicon sequencing*

Chlorophyll extraction was performed in absolute ethanol following standard protocols (Ritchie, 2008; Brito et al., 2009). First, samples were resuspended using a Pasteur pipette, approximately 1–1.5 mL of each sample was transferred to a Macherey & Nagel bead tube and then placed in a bead beater and homogenized for four 60-s cycles each at 40,000 rpm. After homogenization, samples were incubated in the dark for 1 h, then centrifuged at 2500 rpm for 3 min, and 250 µL of the supernatant was transferred into a 96-well plate. The remaining samples were put back at −20 °C for storage. The plate was loaded into a Tecan Infinite M Plex multimode microplate reader (Tecan Group Ltd., Männedorf, Switzerland). The main results from this part of the study were the estimation of photosynthetic biomass using Tecan microplate reader set up in fluorescence bottom reading mode with the following parameters: excitation wavelength at 460 nm, emission wavelength at 680 nm, gain manually set to 135 and 10 flashes per measurement. Chlorophyll fluorescence measurements were saved in an Excel spreadsheet for further statistical analyses.

The preparation and processing of biofilm samples for digital microscopy followed the procedures described by Burfeid-Castellanos et al. (2022). Hydrogen peroxide and hydrochloric acid were used to digest the samples after five prewash cycles (Taylor et al., 2007). The samples were rinsed seven times, centrifuged at 1200 rpm for 3 min (Eppendorf Centrifuge 5427 R; Hamburg, Germany) and decanted with distilled water before they were pipetted onto a coverslip (15 mm × 15 mm, # 1.5), allowed to dry, and then mounted on permanent glass slides with Naphrax resin (refractive index = 1.71, Biologie-Bedarf Thorns, Deggendorf, Germany). To create virtual slides, a 5 mm × 5 mm area on the

permanent glass slide with the highest density of evenly distributed diatom valves was scanned at a magnification of 600× using a VS200 slide scanner (EVIDENT, Tokyo, Japan) with ASW 3.1 software (Olympus Soft Imaging Solutions GmbH, Münster, Germany). A web-browser based image annotation platform, BIIGLE 2.0, was used to count and identify diatoms on these virtual slides (Langenkämper et al., 2017; Burfeid-Castellanos et al., 2022). At least 400 diatom valves were counted and identified up to species level using available literature (Levkov et al., 2013; Trobajo et al., 2013; Cantonati et al., 2017). A list of diatom taxa and their relative abundances was created and utilized for additional analyses.

Sample preparation and DNA extraction for 18S—V9 amplicon sequencing were performed according to Buchner's silica bead-based extraction protocol (Buchner, 2022a, 2022b). Each sample was processed in two replicates, and the genomic DNA amplification of the V9 hypervariable region of the small subunit ribosomal RNA genes (approximately 130 base pairs) was carried out using the universal specific forward primer 1389F (5′-TTGTACACACCGCCC-3′) and the eukaryotic specific reverse primer 1510R (5′-CCTTCYGCAGGTTCACCTAC-3′; Amaral-Zettler et al., 2009), following the protocol described by Stoeck et al. (2010). Sequencing of the resulting libraries was performed on Illumina MiSeq at CeGat GmbH (Tübingen, Germany).

2.3. Bioinformatic analysis of 18S—V9 amplicon sequencing data

The Natrix2 workflow (Welzel et al., 2020; Deep et al., 2023) was used to perform bioinformatic analyses of microphytobenthos Illumina amplicon sequencing data. The workflow's operational taxonomic units (OTUs) variant was implemented using the clustering algorithm Swarm v3.0.0 (Mahé et al., 2015). Paired-end reads were assembled using the simple Bayesian algorithm in PANDAseq v2.11 (Masella et al., 2012). Primers were trimmed using cutadapt v3.2 (Martin, 2011) and filtered with a PANDAseq threshold of 0.9, a minimum length of 77, and a maximum length of 196 nucleotides. Sequence dereplication was performed using the algorithm CD-HIT v4.8.1 (Fu et al., 2012) at 100 % similarity, and chimeric sequences were identified and removed using VSEARCH v2.15.2 (Rognes et al., 2016). The split-sample approach (Lange et al., 2015) was used to reduce erroneous sequences without strict abundance cut-offs. The AmpliconDuo v1.1 R package (Lange et al., 2015) was used for statistical analysis of the amplicon sequencing data resulting from the split-sample process. OTUs were generated by clustering sequences with Swarm v3.0.0 (Mahé et al., 2015) and were then aligned with mothur v1.40.5 (Schloss et al., 2009) against the protist ribosomal reference database (PR^2) v.4.14.0 (Guillou et al., 2013). MUMU (https://github.com/frederic-mahe/mumu), a C++ implementation of LULU (Frøslev et al., 2017), was used for post-clustering curation of the periphyton amplicon sequencing data. The replicates of sequenced samples were merged into one representative sample by calculating the sum of reads for each OTU. The negative controls with the maximum reads were subtracted from the sum of both samples to standardize the sequences' proportions. This step is important to reduce redundancy in the resulting dataset for subsequent statistical analyses. The resulting OTU table was filtered for only eukaryotic algal taxa.

2.4. Statistical analyses

Statistical analyses were performed in R v.4.3.0 (R Core Team, 2023) using the packages 'tidyverse' v2.0.0 (Wickham et al., 2019) and 'vegan' v2.6.4 (Oksanen et al., 2022). Diatom taxa with a relative abundance of at least 1 % were retained for further analysis. For amplicon data, filtering OTUs with read counts below a threshold of >10 vs. no filtering gave similar results in terms of significance; the results given below are from the comparisons of the non-filtered data set. The relative abundance of diatom taxa or OTU was calculated by dividing their count by the total count of the respective sample and then multiplying by 100 to convert it to a percentage. The relative abundances of the dominant diatom taxa and OTU reads were plotted in stacked bar plots and used for further multivariate analyses. Alpha diversity indices, e.g. species richness, Shannon and Simpson, were derived using the 'diversity()' function from 'vegan', based on diatom taxonomy from digital microscopy and microalgae amplicon sequencing. In addition, Gamma and Beta diversity indices, such as Nestedness, Turnover and Sorensen were calculated according to Baselga (2010). These indices and photosynthetic biomass data were compared across treatments using analysis of variance (ANOVA). Next, we conducted individual ANOVAs for each treatment-specific alpha, beta, gamma diversity indices, as well as F_0, Y (II) and standardized Tecan fluorescence measurements using flow velocity, salinity, and temperature as fixed factors. Using the lm() function, linear regression models were fitted with temperature, salinity, flow velocity as the predictor variables and F_0 and Y(II) as the response variables. Due to skewed distributions, Hellinger transformation of the abundance data and OTU reads was performed using the 'decostand()' function of the 'vegan' package to minimize the impact of very abundant taxa and OTUs (Anderson et al., 2006; Legendre and Gallagher, 2001). To determine stressor effects on MPB community composition, 'betadisper()' evaluated multivariate homogeneity of group dispersion and 'adonis2()' executed PERMANOVA. In addition, a pairwise comparison of each treatment against the control was conducted using the 'adonis2()' function to see if they were significantly different. We adjusted *p*-values for multiple comparisons using the Benjamini and Hochberg (1995) method. Associations between samples were visualized with non-metric multidimensional scaling (NMDS) using 'metaMDS()' based on the Bray-Curtis similarity index, with 999 permutations.

3. Results

3.1. Diatom community composition

A total of 257 different diatom taxa belonging to 61 genera were identified during the examination of biofilm samples using digital microscopy. The most dominant taxa in both stressor and recovery samples were *Achnanthidium minutissimum* (52.6 % and 56.5 %, respectively), *Achnanthidium jackii* (9.47 % and 10.65 %, respectively), and *Navicula gregaria* (4.6 % and 4.1 % respectively) of the total valve counts (Fig. 3A). The alpha and gamma diversity indices are listed in Table 3. During the stressor phase, linear regression revealed that both reductions in flow velocity ($t = -2.454$, $p = 0.021$) and increases in temperature ($t = -2.487$, $p = 0.019$) were associated with a significant decrease in the Shannon diversity index, indicating lower biodiversity under these stress conditions. After recovery, mesocosms previously treated with increases in temperature (T) were associated with a significant decrease in Simpson diversity index ($t = -3.329$, $p = 0.002$), suggesting that the lower biodiversity persisted after the increase temperature stress was released. When comparing both the stressor and recovery phases, significantly lower gamma diversity was observed during the recovery phase (ANOVA, $F = 7.4$, $p = 0.02$). Furthermore, we did not detect significant differences in species turnover, nestedness and Sorensen index between treatments during the stressor and recovery phases (all *p*-values >0.05, Table S1).

The analysis of multivariate homogeneity of group dispersions (variances) revealed significant heterogeneity of within-group variances only for the salt treatment (ANOVA, $F = 8.51$, $p = 0.005$). Significant differences in multivariate dispersion were also observed when comparing the two phases of the experiment (ANOVA, $F = 4.583$, $p = 0.036$). PERMANOVA partitioning testing of the effects of temperature, salinity and flow velocity on diatom communities showed a significant effect of temperature ($R^2 = 0.097$, $p = 0.005$) and flow velocity ($R^2 = 0.115$, $p = 0.002$, Table 4) during the stressor phase. A significant effect of temperature was also observed during the recovery phase ($R^2 = 0.094$, $p = 0.002$, Table 4). When testing the effects of experimental phases (stressor vs recovery) and treatments, the phase factor was highly

significant (PERMANOVA, $R^2 = 0.092$, $p = 0.001$), indicating substantial differences in diatom communities between the phases, though a contribution by the heterogeneous dispersions (above) also cannot be excluded. Diatom communities were also significantly different between the treatments ($R^2 = 0.191$, $p = 0.001$, see Table 4), highlighting the influence of treatments on the assemblages. Furthermore, pairwise comparison of each treatment with the control (C) using PERMANOVA revealed a significant effect of increased temperature treatment (T), as well as the combined treatment of reduced flow velocity and increased temperature (F + T) and reduced flow velocity, increased salinity and increased temperature (F + S + T) during the stressor phase (Table S2), that can be summarized as a dominance effect of the temperature treatment. However, after applying corrections for multiple comparisons, all adjusted *p*-values were greater than the significance threshold of 0.05 (Table S2), suggesting that the observed effect may be due to random variation rather than a true effect. The non-metric multidimensional scaling (NMDS) plot showed scattered sample points without a clear treatment-grouping pattern (Fig. 4A).

3.2. Microalgae community composition

18S—V9 amplicon sequencing of microphytobenthos biofilm

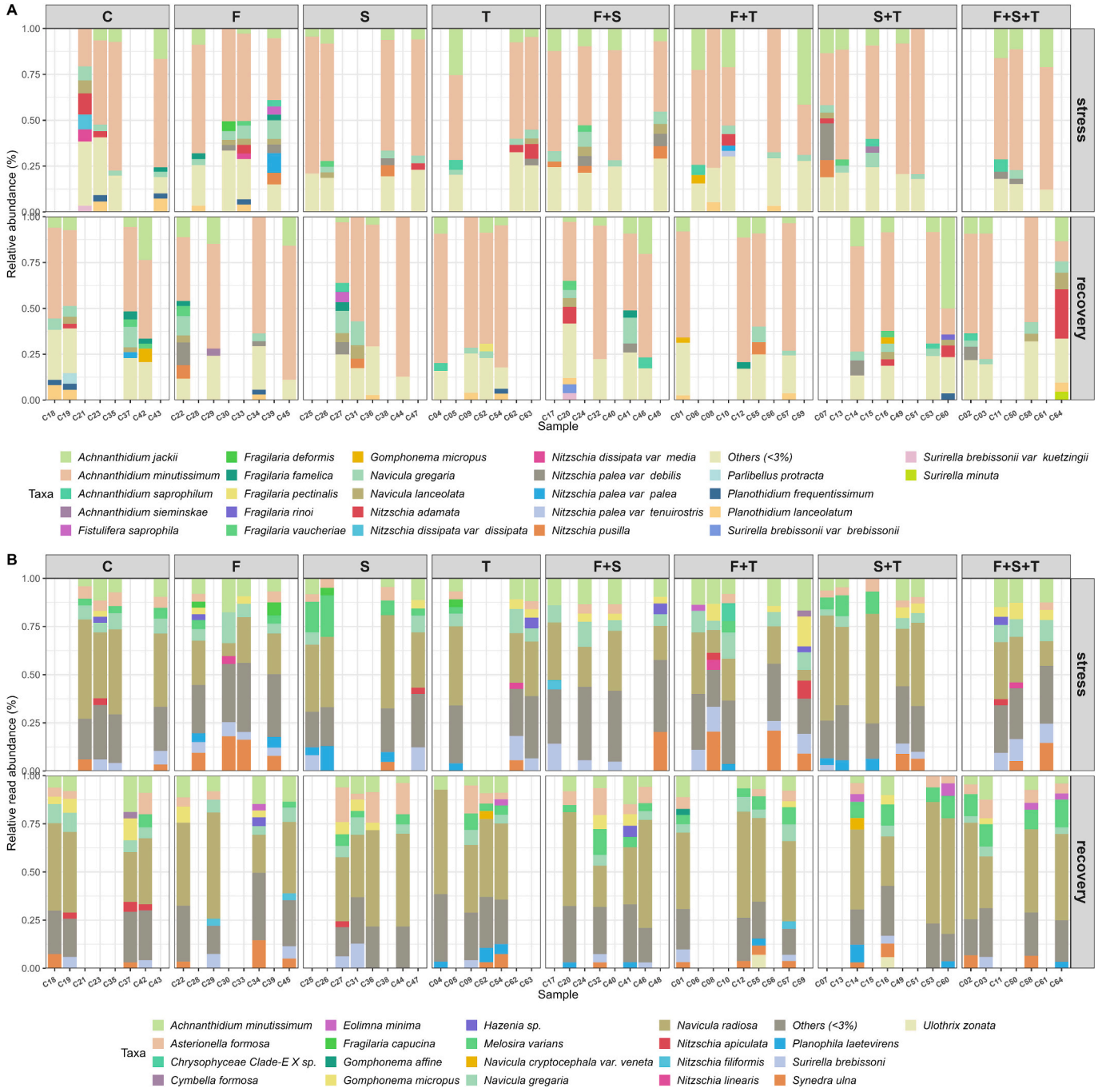

Fig. 3. Community composition of microalgae in different treatments. Relative abundance of the dominant microphytobenthos taxa during stressor and recovery phases. A) Diatom community as determined by digital microscopy. B) OTU read abundance from 18S—V9 amplicon sequencing. C: control; F: reduced flow velocity; S: increased salinity; T: increased temperature; F + S: reduced flow velocity + increased salinity; F + T: reduced flow velocity + increased temperature; S + T: increased salinity + increased temperature; F + S + T: reduced flow velocity + increased salinity + increased temperature. C + numbers (Sample): channel number.

samples, including the recovery samples from the completely scraped areas, generated a total of 34,063,298 reads. Among these reads 785,609 constituting 2.3 % of the total, matched negative controls and were discarded. Following taxonomic filtering, our analysis retained 19,603,405 reads representing 1854 Operational Taxonomic Units (OTUs) in the microalgae dataset. Of these, 13,034,618 reads were obtained from samples collected at the end of both the stress and recovery phases of the experiment, while approximately 6,568,787 reads originated from samples collected from areas that had been entirely stripped of biofilm at the beginning of the recovery phase (henceforth scraped area, to serve as a recolonization area free of priority effects). Diatoms (Bacillariophyta) accounted for 11,696,476 reads, which translates to approximately 89.7 %, of the total microalgae reads, associated with 751 OTUs (Fig. 3B).

The samples obtained from scraped areas exhibited even higher presence of diatoms, with 6,245,423 representing roughly 95 % of the total reads originating from these particular samples (Fig. S2). All samples were dominated by reads of *Achnanthidium minutissimum*, *Asterionella formosa*, *Navicula radiosa*, *Navicula gregaria*, *Gomphonema micropus*, *Ulnaria ulna* and *Surirella brebissonii* (Fig. 3B).

OTU alpha and gamma diversity indices are given in Table 3. During the stressor phase, linear regression revealed significant positive effect of reduced flow velocity on OTUs Shannon ($t = 4.265$, $p < 0.001$) and Simpson (4.757, $p < 0.001$) diversity index, suggesting that reduced flow velocity is associated with higher microalgae diversity. Simpson index was significantly different between the treatments as confirmed by ANOVA ($F = 4.73$, $p = 0.01$). It was lower in mesocosms treated with increased salinity and temperature (S + T) and higher in mesocosms treated with reduced flow velocity (F). Upon comparing the stressor and recovery phases, we observed statistically significant differences in Gamma diversity (ANOVA, $F = 108.7$, $p < 0.001$), OTU richness ($t_{welch} = 10.57$, $p < 0.001$), Shannon index ($t_{welch} = 4.53$, $p < 0.001$) and Simpson index ($t_{welch} = 3.75$, $p < 0.001$), with high mean values often recorded during the stressor phase (Table 3). However, we observed no significant differences in species turnover, nestedness and Sorensen index between the stressor and recovery phase (all $p > 0.05$) (Table S1).

Within-group variances were found to be consistent for all factors tested (ANOVA, all p-values above 0.05). Subsequently, PERMANOVA testing the effects of temperature, salt and flow velocity on microalgae communities showed only a significant effect of flow velocity ($R^2 = 0.144$, $p = 0.001$, Table 4) during the stressor phase. Temperature and salinity had a significant influence on the microalgae community composition during the recovery phase (PERMANOVA, $R^2 = 0.11$, $p = 0.001$ and $R^2 = 0.064$, $p = 0.023$, respectively, Table 4). We also observed significant effects of phase ($R^2 = 0.261$, $p = 0.001$) and treatments ($R^2 = 0.131$, $p = 0.010$). Furthermore, community composition between the scraped and non-scraped surfaces at the end of the recovery phase remained significantly different ($R^2 = 0.161$, $p = 0.001$, Table 4), suggesting priority effects. The comparisons of each treatment with the control confirmed the dominant effect of reduced flow velocity (F) on microalgae OTUs ($R^2 = 0.336$, $p = 0.033$), with a marginal effect of the combined treatment of reduced flow velocity and increased salinity (F + S, $R^2 = 0.295$, $p = 0.046$) and the three applied stressors (F + S + T, $R^2 = 0.255$, $p = 0.049$) during the stressor phase (Table S2). During the recovery phase, the reduced flow velocity and salinity (F + S, $R^2 = 0.297$, $p = 0.029$), reduced flow velocity and temperature (F + T, $R^2 = 0.246$, $p = 0.021$) and reduced flow velocity, salinity and temperature treatment (F + S + T, $R^2 = 0.323$, $p = 0.026$, see Table S2) showed significant effect on microalgae OTUs. However, correction for multiple comparisons resulted in adjusted p-values >0.05, which may indicate random variation rather than true effects of the treatments. The analysis of indicator species revealed that 18 microalgae OTUs were good indicators of increased temperature, nine of which were associated with diatoms. Six OTUs were good indicators of increased salinity, and finally 18 OTUs were good indicators of reduced velocity. The non-metric multidimensional scaling plot (NMDS) showed scattered sampling points with no discernible grouping pattern based on treatments. However, when comparing the two different experimental phases, there was a clear separation between the stressor (dots) and recovery phase (triangles and squares), and between scraped (square) and non-scraped (triangles) areas during the recovery phase (Fig. 4B).

3.3. Photosynthetic biomass and health

Both the minimum and maximum fluorescence intensity (F_0 and Fm) after dark adaptation of the biofilm responded in the same way in all mesocosms during the stressor and recovery phases. Therefore, we present here only the results related to F_0 and maximum quantum yield of Photosystem II (PSII, Y(II) or Fv/Fm), but, Fm data are also shown in Table 5. Analysis of covariance (ANCOVA) revealed that minimum fluorescence intensity (F_0) decreased during the stressor phase ($t = -20.23$, $p < 0.001$). Only temperature was significantly associated with a decrease in F_0 ($t = -3327$, $p < 0.001$) (Fig. 5A). During recovery phase, ANCOVA revealed that flow velocity ($t = 2.7$, $p = 0.007$), temperature ($t = -2.66$, $p = 0.008$), and the interaction term of time in days and flow velocity ($t = -2.451$, $p = 0.015$) were statistically significant (Fig. 5B).

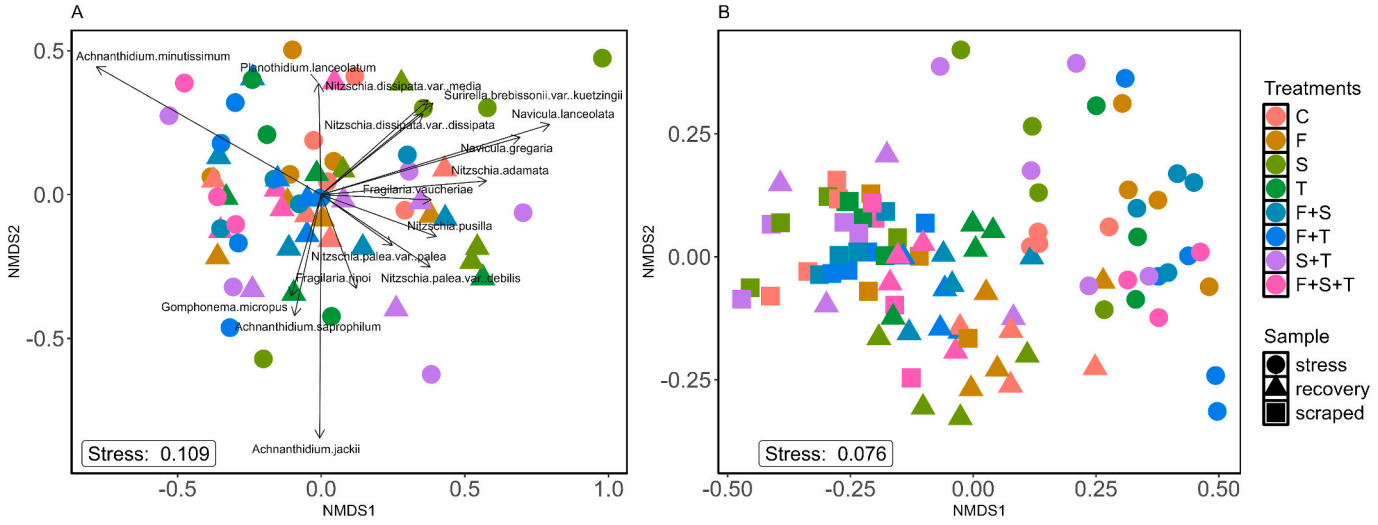

Fig. 4. Non-metric multidimensional scaling plots showing: A) diatom communities from digital microscopy and B) microphytobenthos assemblages as revealed by 18S—V9 amplicon sequencing.

Table 3
Mean Gamma diversity, Richness, Shannon and Simpson diversity indices in different treatments calculated based on digital microscopy and 18S—V9 amplicon sequencing data.

Treat.	Tot. gamma div.	Gamma div.		Richness		Shannon		Simpson	
		Stress	Recov.	Stress	Recov.	Stress	Recov.	stress	Recov.
Diatoms: digital light microscopy									
C	115	92	75	44.50	35.75	2.16	1.79	0.70	0.62
F	106	85	71	42	38.75	1.91	2	0.61	0.68
S	103	85	67	46	35	2.60	2.07	0.82	0.73
T	133	85	92	39.50	41.50	1.86	1.92	0.60	0.66
F + S	111	88	76	40.25	40.75	1.78	2.21	0.61	0.73
F + T	124	92	86	36.50	40.50	1.58	1.73	0.53	0.59
S + T	130	93	91	38.75	44.75	1.84	2.29	0.64	0.76
F + S + T	134	110	76	40.25	39	1.45	1.71	0.50	0.57
Microalgae: 18S—V9 amplicon sequencing									
C	859	697	597	428.25	354.75	2.58	2.57	0.79	0.82
F	851	719	575	448.50	334.25	3.18	2.52	0.91	0.80
S	833	670	558	404.75	303	2.54	2.33	0.81	0.78
T	890	712	620	430	359.25	2.73	2.53	0.86	0.79
F + S	894	746	576	458.50	330	3.06	2.53	0.89	0.80
F + T	920	748	589	430	331.75	2.95	2.38	0.89	0.77
S + T	887	743	534	441.75	302.25	2.56	2.22	0.76	0.72
F + S + T	906	722	596	432.75	335.25	2.89	2.44	0.89	0.79

We observed a strong positive trend ($t = 4.98$, $p < 0.001$) in F_0 over the scraped surfaces during the recovery phase, although with no significant differences by treatment (Fig. 5C). When comparing the scraped with the unscraped areas, ANCOVA showed that the scraped area ($t = -3.878$, $p < 0.001$), flow velocity ($t = 2.832$, $p = 0.005$), temperature (t-value $= -2.795$, $p = 0.005$) and interactions scraped area and time in days ($t = 3.179$, $p = 0.002$) and flow velocity and time in days ($t = -2.569$, $p = 0.01$) had significant effect on F_0 (Fig. 5C).When comparing the scraped with the unscraped areas, the interaction between scraped area and time ($t = 3.179$, $p = 0.002$) may indicate that as the number of days increases, chlorophyll biomass tends to increase, specifically under the condition of recovery after scraping.

The maximum quantum yield of Photosystem II (Y(II) or Fv/Fm) showed a significant ($t = 4.3$, $p < 0.001$) but very small increase (adjusted $R^2 = 0.016$) during the stressor phase, as indicated by the linear regression (Fig. 6A). Y(II) increased significantly over time (t-value 2.118, $p = 0.034$) and with increasing temperature (t-value = 2.419, $p = 0.016$, Fig. 6A). During the recovery phase, Y(II) showed a small but positive trend over time ($t = 2.316$, $p = 0.021$), but no significant effects of all tested predictors (Fig. 6B). These results were also confirmed by ANOVA as all the p-values were also >0.05 (see Table 5). Over the scraped surface, linear regression showed an overall weak but not significant positive trend over time ($t = 1.79$, $p = 0.08$), with no significant effects of flow velocity, increased salinity and temperature, and their interactions (Fig. 6C). When comparing the scraped with the unscraped areas during the recovery phase, only time in days showed significant effects on Y(II) ($t = 2.843$, $p = 0.005$), all the other predictors namely flow velocity, salinity and temperature, and their interactions were not significant. Linear regression showed a positive trend of Y(II) on the final day of the recovery phase on non-scraped areas ($t = 3.33$, $p = 0.001$) and the scraped surfaces ($t = 2.7$, $p = 0.01$). However, the model's overall explanatory power was too small (p adjusted = 0.03). In addition, ANOVA followed by Tukey's multiple comparison test revealed that the mean value of Y(II) was significantly higher in the recovery (unscraped) than in the stressor phases (0.055 units, 95 % CI: 0.016 to 0.094, $p = 0.003$), as well as in the recovery (scraped) than in the stressor phases (0.077 units, 95 % CI: 0.010 to 0.143, $p = 0.02$). However, there was no significant difference between the recovery (scraped) and recovery (unscraped).

3.4. Chlorophyll fluorometry

In our study using Tecan microplate reader to measure chlorophyll fluorescence, we found that there were no significant differences in extracted chlorophyll fluorescence values among the different treatments on the last day of the stressor phase (ANOVA, all $p > 0.05$, Fig. 7). Similarly, when we examined the chlorophyll fluorescence values at the end of the recovery phase, we observed no significant distinction between treatments, as confirmed by our ANOVA analysis (all p values >0.05, Fig. 7). However, when we compared the two experimental phases, we noticed a noteworthy difference in chlorophyll fluorescence levels after the extraction process in the lab. Specifically, the end of the recovery phase exhibited higher chlorophyll fluorescence values ($F = 55.71$, $p < 0.001$), confirming what we observed with in situ chlorophyll fluorescence measurements.

4. Discussion

Our study aimed to unravel the impact of reduction in flow velocity, an increase in salinity and warming water on microphytobenthos communities, focusing on both taxonomic composition and photosynthesis-related functional traits in mesocosms. Our results showed that among 257 diatom taxa identified in this study, *Achnanthidium minutissimum*, *Achnanthidium jackii*, and *Navicula gregaria* were the most dominant in the majority of mesocosms, including the control (C), during the stressor and recovery phases. These taxa are known for their broad ecological range. For example, the prevalence of *A. minutissimum*, which accounted for 54.6 % of total number of counted valves, underlines this wide tolerance range. Taxa from the *A. minutissimum* complex have been reported to be early colonizers or pioneers, often occurring in sites with major anthropogenic impacts (Potapova and Hamilton, 2007; Jüttner et al., 2022). This may be the first indication of a lack of suitable conditions for more sensitive taxa in the system. These pioneer taxa are generally dominant in spring, as this season is characterised by various types of physical disturbances due to flooding and high river flow.

4.1. Stressor effects

4.1.1. Flow velocity

Our study showed that reduced flow velocity significantly influenced the composition, diversity, and biomass of microbial communities. Under reduced flow conditions, diatom-based microscopy assessments

Table 4
Results PERMANOVA testing the effects of temperature, salinity and flow velocity on diatom (digital microscopy) and microalgae (18S—V9 amplicon sequencing) communities df: degrees of freedom; SS: sum of squares; R^2: variance explained by the groups, F: F-statistic, p: p-values, * Significant ($p < 0.05$) main effects and interactions are highlighted in bold.

Factor	*df*	*SS*	R^2	*F*	*Pr (>F)* *
Diatoms: digital microscopy					
Stressor phase					
Temperature	1	0.266	0.097	3.605	**0.001**
Salinity	1	0.078	0.029	1.061	0.356
Velocity	1	0.314	0.115	4.258	**0.002**
Residual	28	2.068	0.753		
Total	31	2.744	1.000		
Recovery phase					
Temperature	1	0.187	0.094	3.187	**0.003**
Salinity	1	0.076	0.038	1.297	0.205
Velocity	1	0.087	0.044	1.492	0.127
Residual	28	1.640	0.824		
Total	31	1.980	1.000		
Phase + treatments					
Phase	1	0.481	0.092	7.075	**0.001**
Treatments	7	0.993	0.191	2.086	**0.001**
Residual	55	3.741	0.718		
Total	63	5.209	1.000		
Algae: 18S—V9 amplicon sequencing					
Stressor phase					
Temperature	1	0.053	0.041	1.465	0.153
Salinity	1	0.037	0.029	1.024	0.344
Velocity	1	0.187	0.144	5.185	**0.001**
Residual	28	1.068	0.753		
Total	31	2.744	1.000		
Recovery phase					
Temperature	1	0.131	0.110	3.851	**0.001**
Salinity	1	0.077	0.064	2.256	**0.023**
Velocity	1	0.033	0.028	0.965	0.455
Residual	28	0.953	0.798		
Total	31	1.194	1.000		
Interactions during recovery					
Temperature:Salinity	1	0.023	0.019	0.687	0.740
Temperature:Velocity	1	0.065	0.054	1.950	**0.039**
Salinity:Velocity	1	0.031	0.026	0.943	0.442
Residual	25	0.834	0.698		
Total	31	1.194	1.000		
Phase + treatments					
Phase	1	0.879	0.261	23.542	**0.001**
Treatments	7	0.440	0.131	1.683	**0.010**
Residual	55	2.054	0.609		
Total	63	3.371	1.000		
Scraped vs unscraped areas during recovery					
Area	1	0.408	0.161	12.695	**0.001**
Treatments	7	0.361	0.142	1.606	**0.007**
Residuals	55	1.767	0.697		
Total	63	2.537	1.000		

revealed a lower Shannon diversity index, indicating a decline in species diversity. In contrast, amplicon sequencing demonstrated a greater Shannon and Simpson diversity index, suggesting an improvement in the microalgae communities' richness. Microscopy and amplicon sequencing revealed that the community composition under reduced flow was significantly different from the other treatments at the end of the stressor and recovery phases, as confirmed by PERMANOVA analyses. Diatom morphology data notably indicate that the difference in community structure continued into the recovery phase. Moreover, under reduced flow conditions compared to other treatments, the minimum fluorescence F_0, a measure of photosynthetic biomass, recovered more quickly. This might indicate that reduced flow has less severe ecophysiological effects on periphyton than temperature or salinity, which is also in line with the observed lack of effect of salinity upon the maximum photosystem II yield (Y(II) or Fv/Fm) of the periphyton.

Table 5
Mean values of photosynthetic biomass (F_0, Fm) and physiological health (Fv/Fm) and ANOVA results comparing each treatment against the control. C: control; T: increased temperature; S: increased salinity; S + T: increased salinity + increased temperature; F: Reduced flow velocity; F + T: reduced flow velocity + increased temperature; F + S: reduced flow + increased salinity; F + S + T: reduced flow velocity + increased salinity + increased temperature; * Significant ($p < 0.05$) main effects and interactions are highlighted in bold.

Treat.	Phase	F_0					Fm					Y(II) or (Fv/Fm)				
		min	max	Estimate	t	p-value*	Min	max	Estimate	t	p-value*	min	Max	Estimate	t	p-value*
C	Stressor	35	1014	246.70	19.55	**<0.001**	120	2660	735.93	21.23	**<0.001**	0.13	0.85	0.65	52.79	**<0.001**
	Recovery	50	563	194.69	16.86	**<0.001**	106	1874	640.25	14.33	**<0.001**	0.09	0.88	0.66	40.85	**<0.001**
T	Stressor	25	679	−39.09	−2.21	**0.03**	75	1452	−121.63	−2.50	**0.01**	0.19	0.88	0.002	0.16	0.87
	Recovery	27	434	−47.46	−2.91	**0.004**	52	1603	−168.74	−2.67	**0.007**	0.11	0.91	−0.02	−0.88	0.38
S	Stressor	41	803	9.31	0.52	0.60	89	2552	−0.54	−0.01	0.99	0	0.88	0.01	0.50	0.62
	Recovery	34	660	−13.07	−0.80	0.43	67	2461	28.11	0.44	0.66	0.44	0.90	0.03	1.442	0.15
S + T	Stressor	18	793	−36.07	−2.03	**0.04**	60	1578	−105.61	−2.17	**0.03**	0.06	0.90	−0.01	−0.44	0.66
	Recovery	33	430	−47.43	−2.89	**0.004**	74	1981	−120.14	−1.89	0.05	0.04	0.84	−0.0008	−0.04	0.97
F	Stressor	32	802	−19.38	−1.09	0.28	106	1807	−63.94	−1.30	0.19	0.03	0.92	−0.02	−1.20	0.23
	Recovery	25	486	−12.65	−0.77	0.44	62	1675	−16.82	−0.27	0.79	0.23	0.87	0.002	0.09	0.93
F + T	Stressor	15	642	39.40	−2.21	**0.03**	50	1614	−154.03	−3.15	**0.001**	0.24	0.87	−0.01	−0.60	0.55
	Recovery	80	522	−24.93	−1.52	0.13	75	1689	−50.00	−0.79	0.43	0.05	0.87	0.03	1.23	0.22
F + S	Stressor	13	758	−24.10	−1.36	0.18	60	2621	−88.50	−1.82	0.06	0	0.886	−0.03	−1.68	0.09
	Recovery	25	407	−2.71	−0.17	0.87	94	1754	2.30	0.04	0.97	0	0.82	0.0002	0.008	0.99
F + S + T	Stressor	19	844	−40.86	−2.29	**0.02**	52	1835	−132.37	−2.71	**0.007**	0.04	0.862	−0.01	−0.29	0.77
	Recovery	54	400	−30.01	−1.82	0.07	112	1725	−87.024	−1.37	0.17	0	0.827	0.0005	0.02	0.98

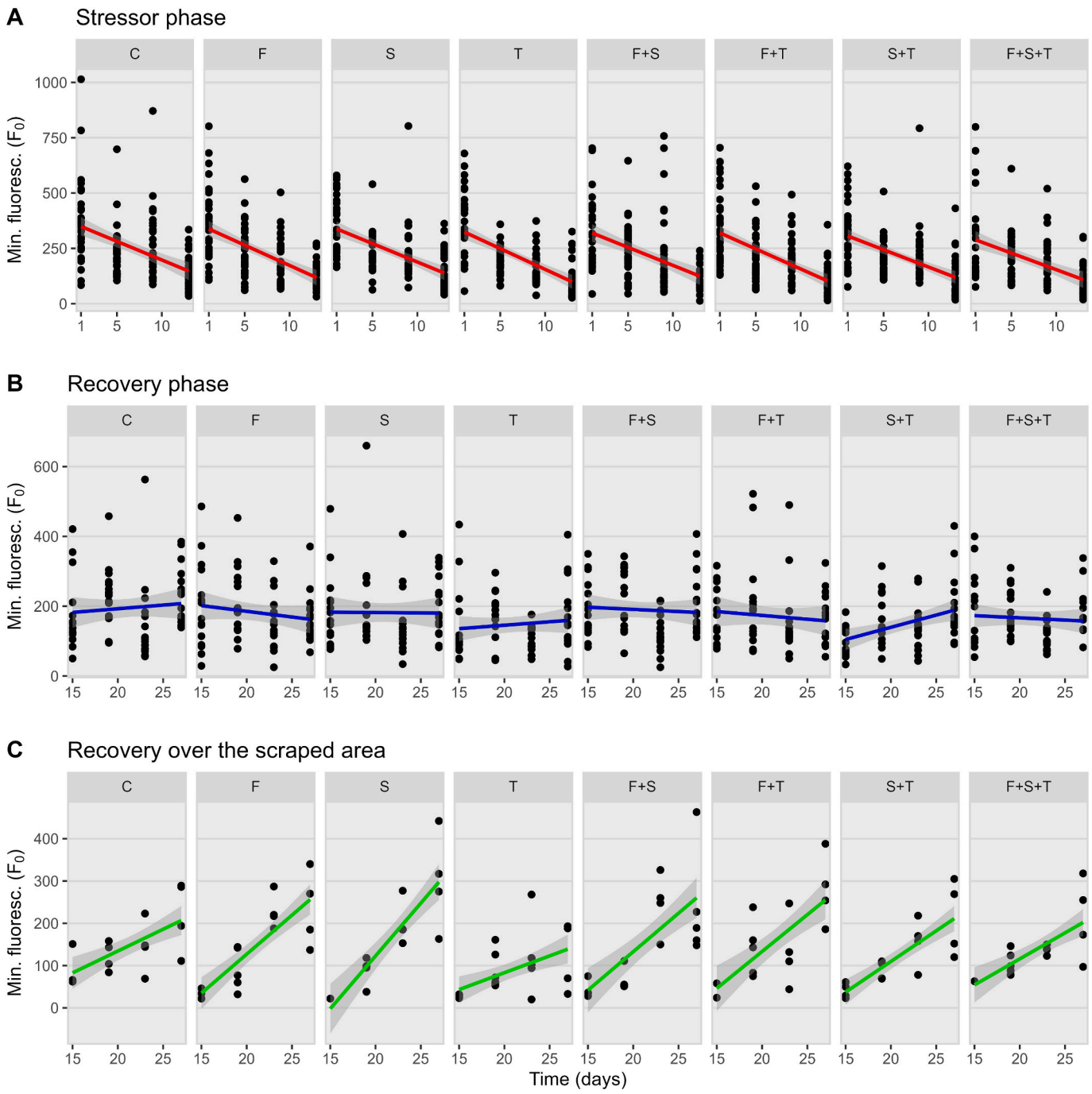

Fig. 5. Plot showing minimum fluorescence yield measurement in different treatments, with fitted linear regression lines. C: control; F: Reduced flow velocity; S: increased salinity; T: increased temperature; F + S: reduced flow + increased salinity; F + T: reduced flow velocity + increased temperature; S + T: increased salinity + increased temperature; F + S + T: reduced flow velocity + increased salinity + increased temperature.

Our amplicon, but not microscopy, results are consistent with previous studies, for example, Salis et al. (2019) found despite decreased flow, there was an increase in taxon richness and a decrease in algal biomass and cell density. Microalgae biofilms growing in slow flow velocity developed visible strands of diatoms and appeared to be thicker and more mature than biofilms in fast flow treatment (Battin et al., 2003a; Battin et al., 2003b; Bondar-Kunze et al., 2016). Rather than community structure, flow-related responses were associated with changes in biomass (Battin et al., 2003b). For example, slower river flow velocities had a major impact on the architecture and dynamics of natural biofilms (Battin et al., 2003b). Nuy et al. (2018) observed only weak community changes as responses to reduced flow velocity. They concluded that flow velocity, despite its known influence on nutrient and oxygen distribution in streams, may not necessarily lead to significant changes in community composition. Furthermore, a weak but significant correlation was found between photosynthetic biomass (F_0) and reduced flow velocity. One quantitative effect of flow velocity was a drop in photosynthetic biomass (Bondar-Kunze et al., 2016).

Summarizing, our analyses of reduced flow conditions revealed inconsistent results about increase / decrease in diversity indices compared to normal flow regimes according to our data, suggesting a decline in diatom biodiversity, alongside an increase in overall algal diversity, under low flow conditions. Furthermore, the composition of diatom and microalgal communities differed significantly under

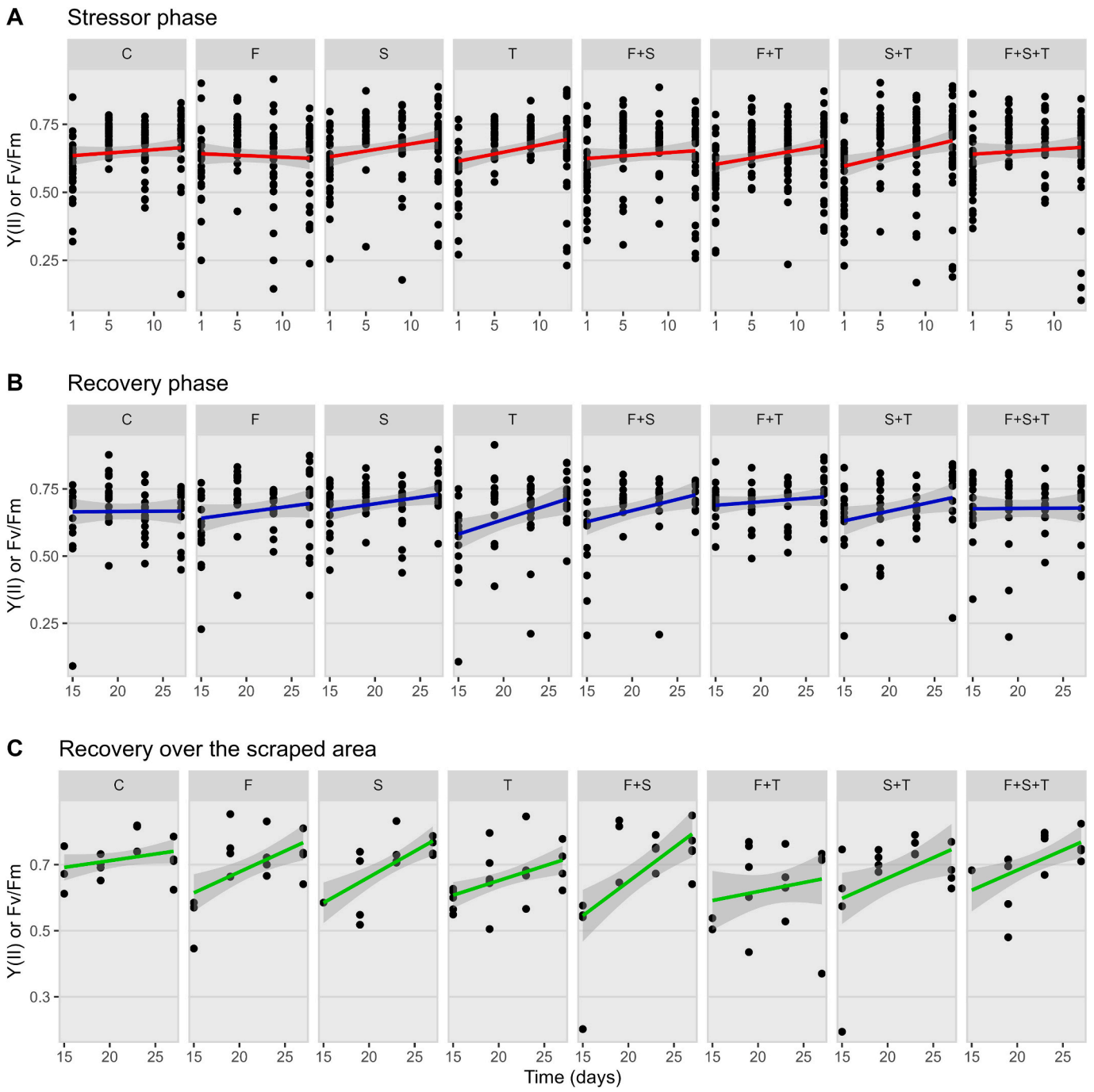

Fig. 6. Plot showing the quantum yield of Photosystem II (Y(II) or Fv/Fm) per treatment with fitted linear regression line. C: control; F: Reduced flow velocity; S: increased salinity; T: increased temperature; F + S: reduced flow + increased salinity; F + T: reduced flow velocity + increased temperature; S + T: increased salinity + increased temperature; F + S + T: reduced flow velocity + increased salinity + increased temperature.

reduced flow conditions compared to other treatments, indicating changes in community structure. Additionally, reduced flow conditions were associated with a slight decrease in photosynthetic biomass, suggesting a possible impact on primary productivity within the ecosystem. These results highlight the importance of considering flow velocity dynamics in understanding and managing aquatic ecosystems, as reductions in flow conditions resulting from low rainfall under climate change scenarios can have significant ecological impacts.

4.1.2. Salinity

We found no significant effect of salinity on microalgae biomass and community composition during stressor phase. This is in contrast to our hypothesis, which predicted a shift in community composition toward a dominance of salt tolerant taxa as a result of increased salinity in the system. However, one diatom taxon and few microalgae OTUs were significant indicators of increased salinity, highlighting their sensitivity as indicators. Microscopy analysis showed that only *Mayamaea permitis* was a significant indicator of increased salinity. This taxon is considered a good indicator of polluted waters (Cantonati et al., 2017). Although microalgae OTUs also showed no statistically significant response to increased salinity treatment during the stressor phase, six (2 Bacillariophyta, 2 Ochrophyta and 2 Chlorophyta) were significant indicators of salinity.

Notably, the average conductivity increase between background and

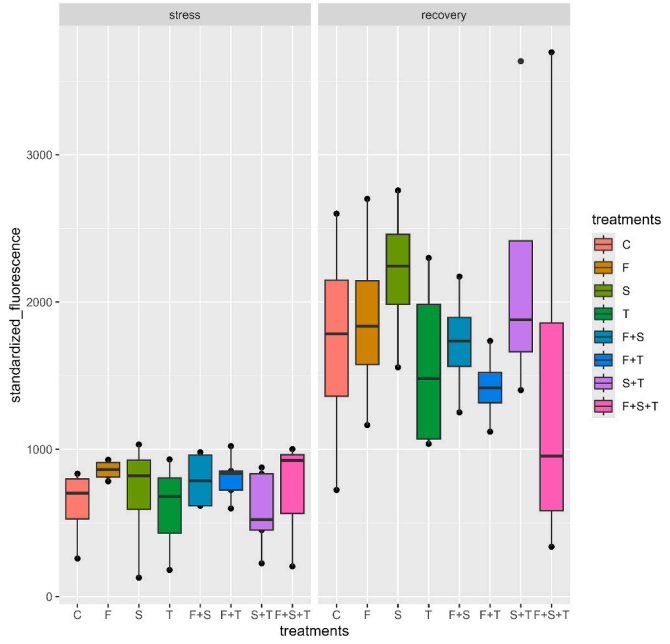

Fig. 7. Boxplot showing chlorophyll fluorescence in different treatments during stressor (Nstr) and recovery (Nrec) phases. C: control (Nstr = 4, Nrec = 4); F: Reduced flow velocity (Nstr = 4, Nrec = 4); S: increased salinity (Nstr = 4, Nrec = 4); T: increased temperature (Nstr = 3, Nrec = 4); F + S: reduced flow + increased salinity (Nstr = 4, Nrec = 4); F + T: reduced flow velocity + increased temperature (Nstr = 5, Nrec = 4); S + T: increased salinity + increased temperature (Nstr = 5, Nrec = 4); F + S + T: reduced flow velocity + increased salinity + increased temperature (Nstr = 3, Nrec = 4).

increased salinity treatment was 0.529 mS/cm, corresponding to an added chloride of 154 mg/L. Although in general, even an increase of chloride concentration by 0.5 mg/L can lead to a change in the structure of microalgae community (Stenger-Kovács et al., 2023), the stream investigated here regularly experiences salinity fluctuations that are substantially larger than we could simulate in our mesocosm experiment. Our results show that the salinity increase by ca. 154 mg/L did not constitute a significant stressor in the studied ecosystem. In spite of this, both microscopic and amplicon analyses revealed subtle but noticeable differences compared to control conditions. Altogether, salinity change of the magnitude applied here may be a subliminal stressor for the studied system, with only a few diatom and microalgal species responding, also highlighting the sensitivity of the few affected taxa as indicators of salinity change.

4.1.3. Temperature

We detected a significant effect of increased temperature treatment on diatom communities (Shannon diversity and taxonomic composition as determined by microscopy) but not on the whole microalgae assemblages (amplicon data). *Parlibellus protractoides* and *Fragilaria pectinalis* were good indicators of increase in temperature. Shannon diversity was lower in increased temperature mesocosms, in line with our hypothesis. Often, stressors cause a decline in diatom species richness as observed in this case with increasing temperature in mesocosms (Piggott et al., 2015; Da Silva et al., 2019; Lengyel et al., 2023b). In this study, we achieved stressor treatment by effectively increasing temperature for at least 9 days of warming. According to Lengyel et al. (2023b), a moderate temperature increase of 3 °C may be the main factor changing the composition of benthic algal community. It is important to note that this study was conducted in the summer with temperatures above 20 °C, making direct comparisons difficult as our study took place in the spring with the highest mean ambient temperature of 8.7 °C. Thus, our temperature increase treatment of +3.45 °C kept stressed mesocosms within the optimal range for the growth of diatoms. This probably favoured diatom growth since they usually prefer lower temperatures, having their optimum growth below 20 °C (Patrick et al., 1969). Although some diatoms can grow even at higher temperatures, they cannot compete with Cyanobacteria, due to their better resource utilization and, in some cases, production of allelochemicals (Leflaive and Ten-Hage, 2007). Many diatoms have an optimal growth temperature range between 5 and 20 °C, Chlorophyta between 15 and 30 °C and Cyanobacteria can also grow above 30 °C (Patrick et al., 1969). Therefore, to better simulate critical ecological effects of global warming, heated stream mesocosm experiments conducted in summer will be more suitable.

While photosynthetic biomass (F_0) decreased in all mesocosms during the stressor phase, the maximum quantum yield (Y(II) or Fv/Fm) showed a slight increase, with increased temperature showing a weak positive effect. The initial decrease in photosynthetic biomass could be due to an overall strong cooling during the stressor phase, which may have overridden treatment effects on overall periphyton growth (as seen in F_0). Contrary to Lengyel et al. (2023b), who found that higher temperature reduced the maximum quantum yield of photosystem II in microphytobenthos, we found a positive effect; the difference between both studies can again probably be explained by the different ambient temperatures.

4.1.4. Stressor interactions

Our results showed only one statistically significant interaction between temperature and flow velocity, which had a small but significant positive coefficient. This suggests a potentially synergistic effect between these two variables on microalgae OTUs. Thus, the combined influence of velocity and temperature may affect microalgae communities more than would be predicted from the effect of each variable acting alone (Vos et al., 2023). Synergistic interactions underscore the complexity of ecological interactions in stream ecosystems and highlight the importance of considering multiple environmental factors when assessing their impact on microalgae communities. There was no other significant two- or three-way interaction.

4.2. Recovery

Several observations (e.g. differences in multivariate dispersions, Gamma and Beta diversity indices, Table S1) indicate a homogenization of diatom communities during the recovery phase in comparison with the stressor phase. This is expected due to the more similar environmental conditions. Most treatment channels reached a recovery end time point community composition statistically indistinguishable from the control channels, indicating a close-to-complete recovery during the 2-week recovery phase (Table S2). Fluctuations in temperature likely played a significant role in shaping the composition and dynamics of periphyton communities and biomass during our experiment and the rather different ambient temperatures are suspected to play an important role in explaining this.

4.3. Priority effects

We observed faster microphytobentos growth on scraped surfaces compared to those on unscraped ones during the recovery phase, resulting in identical total in vivo chlorophyll fluorescence (as a proxy of photosynthetic biomass) at the end of the recovery phase. Community composition after the two weeks of the recovery phase was different in the scraped when compared with the non-scraped areas. This observation suggests that substrate occupancy by resident taxa slowed down recolonization after stressor effect, and influenced the taxonomic composition of the final communities. We interpret this to reflect transitional priority effects caused by competition for substrate between resident and immigrant taxa (Stroud et al., 2024). Further research into the mechanisms driving priority effects in microphytobenthos communities could provide valuable insights into asymmetric paths of recovery

vs degradation.

5. Conclusion

This study examined the response of microalgae to reduction in flow velocity, and increase in salinity and temperature in a stream mesocosm experiment. We detected significant effects of flow velocity and temperature on microalgae communities, increase in salinity led to little change, probably because the applied stressor intensity was relatively mild for microphytobenthic organisms of the study system. Although we saw a rough convergence among stressor treatments during the recovery phase of the experiment, the different communities observed between pre-colonized vs. cleaned (scraped) areas at the recovery end time point indicate that a successional climax has probably not been reached by this time. The latter comparison also indicates that resident communities at least transiently influence recolonization dynamics in a post-stressor recovery, in line with the Asymmetric Response Concept (Vos et al., 2023).

Supplementary data to this article can be found online at https://doi.org/10.1016/j.scitotenv.2024.173670.

CRediT authorship contribution statement

Ntambwe Albert Serge Mayombo: Writing – review & editing, Writing – original draft, Visualization, Validation, Software, Investigation, Formal analysis, Data curation, Conceptualization. **Andrea M. Burfeid-Castellanos:** Writing – review & editing, Writing – original draft, Supervision, Resources, Project administration, Conceptualization. **Anna-Maria Vermiert:** Writing – review & editing, Project administration, Methodology, Investigation. **Iris Madge Pimentel:** Writing – review & editing, Visualization, Project administration, Methodology, Investigation, Data curation. **Philipp M. Rehsen:** Writing – review & editing, Project administration, Methodology, Investigation, Conceptualization. **Mimoza Dani:** Writing – review & editing, Investigation. **Christina Jasinski:** Writing – review & editing, Investigation. **Marzena Agata Spyra:** Writing – review & editing, Project administration, Investigation. **Michael Kloster:** Writing – review & editing, Software, Project administration, Methodology, Investigation. **Danijela Vidaković:** Writing – review & editing, Investigation. **Dominik Buchner:** Writing – review & editing, Project administration, Methodology, Investigation. **Bánk Beszteri:** Writing – review & editing, Supervision, Project administration, Funding acquisition, Conceptualization.

Declaration of competing interest

The authors declare no conflict of interest.

Data availability

All the datasets and the R scripts used in this study are available in our GitHub repository: https://github.com/sergemayombo/exstream2022.

Acknowledgements

This study was conducted within framework of the Collaborative Research Centre (CRC) 1439 RESIST (Multilevel Response to Stressor Increase and Decrease in Stream Ecosystems; www.sfb-resist.de) funded by the Deutsche Forschungsgemeinschaft (DFG, German Research Foundation; CRC 1439/1, project number: 426547801). We are very grateful for the support of many helpers during the experiment in the field and laboratory work. The editor and two anonymous reviewers are thanked for their comments that helped improve this manuscript. We acknowledge support by the Open Access Publication Fund of the University of Duisburg-Essen.

References

Amaral-Zettler, L.A., McCliment, E.A., Ducklow, H.W., Huse, S.M., 2009. A method for studying protistan diversity using massively parallel sequencing of V9 hypervariable regions of small-subunit ribosomal RNA genes. PloS One 4 (7), e6372. https://doi.org/10.1371/journal.pone.0006372.

Anderson, M.J., Ellingsen, K.E., McArdle, B.H., 2006. Multivariate dispersion as a measure of beta diversity. Ecol. Lett. 9 (6), 683–693. https://doi.org/10.1111/j.1461-0248.2006.00926.x.

Baselga, A., 2010. Partitioning the turnover and nestedness components of beta diversity. Glob. Ecol. Biogeogr. 19 (1), 134–143. https://doi.org/10.1111/j.1466-8238.2009.00490.x.

Battin, T.J., Kaplan, L.A., Denis Newbold, J., Hansen, C.M.E., 2003a. Contributions of microbial biofilms to ecosystem processes in stream mesocosms. Nature 426 (6965), 439–442. https://doi.org/10.1038/nature02152.

Battin, T.J., Kaplan, L.A., Newbold, J.D., Cheng, X., Hansen, C., 2003b. Effects of current velocity on the nascent architecture of stream microbial biofilms. Appl. Environ. Microbiol. 69 (9), 5443–5452. https://doi.org/10.1128/AEM.69.9.5443-5452.2003.

B-Béres, V., Stenger-Kovács, C., Buczkó, K., Padisák, J., Selmeczy, G.B., Lengyel, E., Tapolczai, K., 2023. Ecosystem services provided by freshwater and marine diatoms. Hydrobiologia 850 (12–13), 2707–2733. https://doi.org/10.1007/s10750-022-04984-9.

Benjamini, Y., Hochberg, Y., 1995. Controlling the false discovery rate: a practical and powerful approach to multiple testing. J. R. Stat. Soc. Series B Stat. Methodology 57 (1), 289–300. https://doi.org/10.1111/j.2517-6161.1995.tb02031.x.

Bondar-Kunze, E., Maier, S., Schönauer, D., Bahl, N., Hein, T., 2016. Antagonistic and synergistic effects on a stream periphyton community under the influence of pulsed flow velocity increase and nutrient enrichment. Sci. Total Environ. 573, 594–602. https://doi.org/10.1016/j.scitotenv.2016.08.158.

Bondar-Kunze, E., Kasper, V., Hein, T., 2021. Responses of periphyton communities to abrupt changes in water temperature and velocity, and the relevance of morphology: a mesocosm approach. Sci. Total Environ. 768, 145200 https://doi.org/10.1016/j.scitotenv.2021.145200.

Brito, A., Newton, A., Tett, P., Fernandes, T., 2009. Development of an optimal methodology for the extraction of microphytobenthic chlorophyll. J. Int. Environ. Appl. Sci. 4(1, 42–54. Available online at. https://sapientia.ualg.pt/handle/10400.1/1098.

Brown, S., Manoylov, K.M., 2023. Assessing diatom community dynamics in a recovering agricultural stream in middle Georgia, USA. Phycology 3 (2), 294–304. https://doi.org/10.3390/phycology3020019.

Buchner, D., 2022a. Sample preparation and lysis of homogenized malaise trap samples v1. https://www.protocols.io/view/sample-preparation-and-lysis-of-homogenized-malais-dm6gpjrmjgzp/v1.

Buchner, D., 2022b. Guanidine-based DNA extraction with silica-coated beads or silica spin columns v2. https://www.protocols.io/view/guanidine-based-dna-extraction-with-silica-coated-eq2ly73mmlx9/v2.

Burfeid-Castellanos, A.M., Kloster, M., Beszteri, S., Postel, U., Spyra, M., Zurowietz, M., et al., 2022. A digital light microscopic method for diatom surveys using embedded acid-cleaned samples. Water 14 (20), 3332. https://doi.org/10.3390/w14203332.

Cañedo-Argüelles, M., Kefford, B.J., Piscart, C., Prat, N., Schäfer, R.B., Schulz, C.-J., 2013. Salinisation of rivers: an urgent ecological issue. Environ. Pollut. (Barking, Essex : 1987) 173, 157–167. https://doi.org/10.1016/j.envpol.2012.10.011.

Cantonati, M., Kelly, M.G., Lange-Bertalot, H. (Eds.), 2017. Freshwater Benthic Diatoms of Central Europe. Over 800 Common Species Used in Ecological Assessment; Engl. Ed. with Updated Taxonomy and Added Species. Koeltz Botanical Books, Schmitten-Oberreifenberg.

Castillo, A.M., Sharpe, D.M.T., Ghalambor, C.K., de León, L.F., 2018. Exploring the effects of salinization on trophic diversity in freshwater ecosystems: a quantitative review. Hydrobiologia 807 (1), 1–17. https://doi.org/10.1007/s10750-017-3403-0.

Costello, D.M., Kulacki, K.J., McCarthy, M.E., Tiegs, S.D., Cardinale, B.J., 2018. Ranking stressor impacts on periphyton structure and function with mesocosm experiments and environmental-change forecasts. PloS One 13 (9), e0204510. https://doi.org/10.1371/journal.pone.0204510.

Cunillera-Montcusí, D., Beklioğlu, M., Cañedo-Argüelles, M., Jeppesen, E., Ptacnik, R., Amorim, C.A., et al., 2022. Freshwater salinisation: a research agenda for a saltier world. Trends Ecol. Evol. 37 (5), 440–453. https://doi.org/10.1016/j.tree.2021.12.005.

Da Silva, C.F.M., Torgan, L.C., Schneck, F., 2019. Temperature and surface runoff affect the community of periphytic diatoms and have distinct effects on functional groups: evidence of a mesocosms experiment. Hydrobiologia 839 (1), 37–50. https://doi.org/10.1007/s10750-019-03992-6.

Deep, A., Bludau, D., Welzel, M., Clemens, S., Heider, D., Boenigk, J., Beisser, D., 2023. Natrix2 – Improved amplicon workflow with novel Oxford Nanopore Technologies support and enhancements in clustering, classification and taxonomic databases. MBMG 7, e109389. https://doi.org/10.3897/mbmg.7.109389.

Dixit, S.S., Smol, J.P., Charles, D.F., Hughes, R.M., Paulsen, S.G., Collins, G.B., 1999. Assessing water quality changes in the lakes of the northeastern United States using sediment diatoms. Can. J. Fish. Aquat. Sci. 56 (1), 131–152. https://doi.org/10.1139/f98-148.

Duong, T.T., Coste, M., Feurtet-Mazel, A., Dang, D.K., Ho, C.T., Le, T.P.Q., 2012. Responses and structural recovery of periphytic diatom communities after short-term disturbance in some rivers (Hanoi, Vietnam). J. Appl. Phycol. 24 (5), 1053–1065. https://doi.org/10.1007/s10811-011-9733-9.

European Commission, 2000. Directive 2000/60/EC of the European parliament and of the council of 23 October 2000 establishing a framework for community action in the field of water policy. Off. J. Eur. Commun. L327 (1–72).

Frøslev, T.G., Kjøller, R., Bruun, H.H., Ejrnæs, R., Brunbjerg, A.K., Pietroni, C., Hansen, A. J., 2017. Algorithm for post-clustering curation of DNA amplicon data yields reliable biodiversity estimates. Nat. Commun. 8 (1), 1188. https://doi.org/10.1038/s41467-017-01312-x.

Frost, C., Tibby, J., Goonan, P., 2023. Diatom–salinity thresholds in experimental outdoor streams reinforce the need for stricter water quality guidelines in South Australia. Hydrobiologia 850 (14), 2991–3011. https://doi.org/10.1007/s10750-023-05163-0.

Fu, L., Niu, B., Zhu, Z., Wu, S., Li, W., 2012. CD-HIT: accelerated for clustering the next-generation sequencing data. Bioinformatics (Oxford, England) 28 (23), 3150–3152. https://doi.org/10.1093/bioinformatics/bts565.

Guillou, L., Bachar, D., Audic, S., Bass, D., Berney, C., Bittner, L., et al., 2013. The Protist ribosomal reference database (PR2): a catalog of unicellular eukaryote small sub-unit rRNA sequences with curated taxonomy. Nucleic Acids Res. 41 (Database issue), D597–D604. https://doi.org/10.1093/nar/gks1160.

Heikkinen, J.M., Aalto, J., Rantamäki, O., Ruikkala, T., Soininen, J., Pajunen, V., 2022. Observing diatom diversity and community composition along environmental gradients in subarctic mountain ponds. Freshw. Biol. 67 (4), 731–741. https://doi.org/10.1111/fwb.13877.

Hering, D., Johnson, R.K., Kramm, S., Schmutz, S., Szoszkiewicz, K., Verdonschot, P.F. M., 2006. Assessment of European streams with diatoms, macrophytes, macroinvertebrates and fish: a comparative metric-based analysis of organism response to stress. Freshw. Biol. 51 (9), 1757–1785. https://doi.org/10.1111/j.1365-2427.2006.01610.x.

Honeywill, C., Paterson, D., Hagerthey, S., 2002. Determination of microphytobenthic biomass using pulse-amplitude modulated minimum fluorescence. Eur. J. Phycol. 37 (4), 485–492. https://doi.org/10.1017/S0967026202003888.

Jüttner, I., Hamilton, P.B., Wetzel, C.E., van Vijver, B. de, King, L., Kelly, M.G., et al., 2022. A study of the morphology and distribution of four Achnanthidium Kütz. Species (Bacillariophyta), implications for ecological status assessment, and description of two New European Species. Cryptogamie, Algologie 43 (10). https://doi.org/10.5252/cryptogamie-algologie2022v43a10.

Kelly, M.G., Free, G., Kolada, A., Phillips, G., Warner, S., Wolfram, G., Poikane, S., 2023. Warding off freshwater salinization: Do current criteria measure up? WIREs Water, e1694. https://doi.org/10.1002/wat2.1694.

Lacoursière, S., Lavoie, I., Rodríguez, M.A., Campeau, S., 2011. Modeling the response time of diatom assemblages to simulated water quality improvement and degradation in running waters. Can. J. Fish. Aquat. Sci. 68 (3), 487–497. https://doi.org/10.1139/F10-162.

Lange, Anja, Jost, Steffen, Heider, Dominik, Bock, Christina, Budeus, Bettina, Schilling, Elmar, et al., 2015. AmpliconDuo: a Split-sample filtering protocol for high-throughput amplicon sequencing of microbial communities. PLOS ONE 10 (11), e0141590. https://doi.org/10.1371/journal.pone.0141590.

Langenkämper, D., Zurowietz, M., Schoening, T., Nattkemper, T.W., 2017. BIIGLE 2.0 - browsing and annotating large marine image collections. Front. Mar. Sci. 4, Article 83 https://doi.org/10.3389/fmars.2017.00083.

Leflaive, J., Ten-Hage, L., 2007. Algal and cyanobacterial secondary metabolites in freshwaters: a comparison of allelopathic compounds and toxins. Freshw. Biol. 52 (2), 199–214. https://doi.org/10.1111/j.1365-2427.2006.01689.x.

Legendre, P., Gallagher, E.D., 2001. Ecologically meaningful transformations for ordination of species data. Oecologia 129 (2), 271–280. https://doi.org/10.1007/s004420100716.

Lengyel, E., Barreto, S., Padisák, J., Stenger-Kovács, C., Lázár, D., Buczkó, K., 2023a. Contribution of silica-scaled chrysophytes to ecosystems services: a review. Hydrobiologia 850 (12–13), 2735–2756. https://doi.org/10.1007/s10750-022-05075-5.

Lengyel, E., Stenger-Kovács, C., Boros, G., Al-Imari, T.J.K., Novák, Z., Bernát, G., 2023b. Anticipated impacts of climate change on the structure and function of phytobenthos in freshwater lakes. Environ. Res. 238 (Pt 2), 117283 https://doi.org/10.1016/j.envres.2023.117283.

Levkov, Z., Metzeltin, D., Pavlov, A. (Eds.), 2013. Luticola and Luticolopsis. In Diatoms of the European Inland Waters and Comparable Habitats P. 698. With Assistance of Bertalot, H.L., Ed, 1st ed. Koeltz Botanical Books, Oberreifenberg, Germany.

Lobo, E.A., Heinrich, C.G., Schuch, M., Wetzel, C.E., Ector, L., 2016. Diatoms as Bioindicators in Rivers. In Orlando Necchi JR (Ed.): River Algae [recurso electrónico]. Cham: Springer, Cham, pp. 245–271. https://doi.org/10.1007/978-3-319-31984-1_11.

Mahé, F., Rognes, T., Quince, C., Vargas, C., de M., Dunthorn, 2015. Swarm v2: highly-scalable and high-resolution amplicon clustering. PeerJ 3, e1420. https://doi.org/10.7717/peerj.1420.

Mandalakis, M., Stravinskaitė, A., Lagaria, A., Psarra, S., Polymenakou, P., 2017. Ultrasensitive and high-throughput analysis of chlorophyll a in marine phytoplankton extracts using a fluorescence microplate reader. Anal. Bioanal. Chem. 409 (19), 4539–4549. https://doi.org/10.1007/s00216-017-0392-9.

Marcel, R., Berthon, V., Castets, V., Rimet, F., Thiers, A., Labat, F., Fontan, B., 2017. Modelling diatom life forms and ecological guilds for river biomonitoring. Knowl. Manag. Aquat. Ecosyst. 418, 1. https://doi.org/10.1051/kmae/2016033.

Martin, M., 2011. Cutadapt removes adapter sequences from high-throughput sequencing reads. EMBnet J. 17 (1), 10. https://doi.org/10.14806/ej.17.1.200.

Masella, A.P., Bartram, A.K., Truszkowski, J.M., Brown, D.G., Neufeld, J.D., 2012. PANDAseq: paired-end assembler for illumina sequences. BMC Bioinform. 13 (1), 31. https://doi.org/10.1186/1471-2105-13-31.

Nuy, J.K., Lange, A., Beermann, A.J., Jensen, M., Elbrecht, V., Röhl, O., et al., 2018. Responses of stream microbes to multiple anthropogenic stressors in a mesocosm study. Sci. Total Environ. 633, 1287–1301. https://doi.org/10.1016/j.scitotenv.2018.03.077.

Oksanen, J., Simpson, G., Blanchet, F., Kindt, R., Legendre, P., Minchin, P., O'Hara, R., Solymos, P., Stevens, M., Szoecs, E., et al., 2022. Package 'vegan'. Version 2.6-4. Available online at. http://cran.ism.ac.jp/web/packages/vegan/vegan.pdf.

Patrick, R., Crum, B., Coles, J., 1969. Temperature and manganese as determining factors in the presence of diatom or blue-green algal floras in streams. Proc. Nat. Acad. Sci. USA 64 (2), 472–478. https://doi.org/10.1073/pnas.64.2.472.

Peterson, C.G., Hoagland, K.D., Stevenson, R.J., 1990. Timing of wave disturbance and the resistance and recovery of a freshwater Epilithic microalgal community. J. North Am. Benthol. Soc. 9 (1), 54–67. https://doi.org/10.2307/1467934.

Piggott, J.J., Salis, R.K., Lear, G., Townsend, C.R., Matthaei, C.D., 2015. Climate warming and agricultural stressors interact to determine stream periphyton community composition. Glob. Change Biol. 21 (1), 206–222. https://doi.org/10.1111/gcb.12661.

Potapova, M., Hamilton, P.B., 2007. Morphological and ecological variation within the Achnanthidium minutissimum (Bacillariophyceae) species complex 1. J. Phycol. 43 (3), 561–575. https://doi.org/10.1111/j.1529-8817.2007.00332.x.

R Core Team (2023): R: A Language and Environment for Statistical Computing. Vienna, Austria. Available online at https://www.R-project.org/.

Ritchie, R.J., 2008. Universal chlorophyll equations for estimating chlorophylls a, b, c, and d and total chlorophylls in natural assemblages of photosynthetic organisms using acetone, methanol, or ethanol solvents. Photosynthetica 46 (1), 115–126. https://doi.org/10.1007/s11099-008-0019-7.

Rognes, T., Flouri, T., Nichols, B., Quince, C., Mahé, F., 2016. VSEARCH: a versatile open source tool for metagenomics. PeerJ 4, e2584. https://doi.org/10.7717/peerj.2584.

Salis, R.K., Bruder, A., Piggott, J.J., Summerfield, T.C., Matthaei, C.D., 2019. Multiple-stressor effects of dicyandiamide (DCD) and agricultural stressors on trait-based responses of stream benthic algal communities. Sci. Total Environ. 693, 133305 https://doi.org/10.1016/j.scitotenv.2019.07.111.

Schloss, P.D., Westcott, S.L., Ryabin, T., Hall, J.R., Hartmann, M., Hollister, E.B., et al., 2009. Introducing mothur: open-source, platform-independent, community-supported software for describing and comparing microbial communities. Appl. Environ. Microbiol. 75 (23), 7537–7541. https://doi.org/10.1128/AEM.01541-09.

Schreiber, U., 1986. Detection of rapid induction kinetics with a new type of high-frequency modulated chlorophyll fluorometer. Photosyn. Res. 9 (1–2), 261–272. https://doi.org/10.1007/BF00029749.

Schröder, M., Sondermann, M., Sures, B., Hering, D., 2015. Effects of salinity gradients on benthic invertebrate and diatom communities in a German lowland river. Ecol. Indic. 57, 236–248. https://doi.org/10.1016/j.ecolind.2015.04.038.

Siegel, P., Baker, K.G., Low-Décarie, E., Geider, R.J., 2023. Phytoplankton competition and resilience under fluctuating temperature. Ecol. Evol. 13 (3), e9851 https://doi.org/10.1002/ece3.9851.

Silva, E.I.L., 2000. Salt pollution in a Japanese stream and its effects on water chemistry and epilithic algal chlorophyll-a. Hydrobiologia 437 (1/3), 139–148. https://doi.org/10.1023/A:1026598723329.

Steinman, A.D., McIntire, C.D., 1990. Recovery of lotic periphyton communities after disturbance. Environ. Manag. 14 (5), 589–604. https://doi.org/10.1007/BF02394711.

Stenger-Kovács, C., Béres, V.B., Buczkó, K., Tapolczai, K., Padisák, J., Selmeczy, G.B., Lengyel, E., 2023. Diatom community response to inland water salinization: a review. Hydrobiologia 850 (20), 4627–4663. https://doi.org/10.1007/s10750-023-05167-w.

Stoeck, T., Bass, D., Nebel, M., Christen, R., Jones, M.D.M., Breiner, H.-W., Richards, T. A., 2010. Multiple marker parallel tag environmental DNA sequencing reveals a highly complex eukaryotic community in marine anoxic water. Mol. Ecol. 19 (Suppl. 1), 21–31. https://doi.org/10.1111/j.1365-294X.2009.04480.x.

Striebel, M., Schabhüttl, S., Hodapp, D., Hingsamer, P., Hillebrand, H., 2016. Phytoplankton responses to temperature increases are constrained by abiotic conditions and community composition. Oecologia 182 (3), 815–827. https://doi.org/10.1007/s00442-016-3693-3.

Stroud, J.T., Delory, B.M., Barnes, E.M., Chase, J.M., de Meester, L., Dieskau, J., et al., 2024. Priority effects transcend scales and disciplines in biology. Trends Ecol. Evol. 3279 https://doi.org/10.1016/j.tree.2024.02.004.

Taylor, J.C., Harding, W.R., Archibald, C.G.M., 2007. A Methods Manual For The Collection, Preparation And Analysis Of Diatom Samples.

Tonkin, J.D., Merritt, D.M., Olden, J.D., Reynolds, L.V., Lytle, D.A., 2018. Flow regime alteration degrades ecological networks in riparian ecosystems. Nat. Ecol. Evol. 2 (1), 86–93. https://doi.org/10.1038/s41559-017-0379-0.

Trobajo, R., Rovira, L., Ector, L., Wetzel, C.E., Kelly, M., Mann, D.G., 2013. Morphology and identity of some ecologically important small Nitzschia species. Diat. Res. 28 (1), 37–59. https://doi.org/10.1080/0269249X.2012.734531.

Virtanen, L., Soininen, J., 2012. The roles of environment and space in shaping stream diatom communities. Eur. J. Phycol. 47 (2), 160–168. https://doi.org/10.1080/09670262.2012.682610.

Vos, M., Hering, D., Gessner, M.O., Leese, F., Schäfer, R.B., Tollrian, R., et al., 2023. The asymmetric response concept explains ecological consequences of multiple stressor exposure and release. Sci. Total Environ. 872, 162196 https://doi.org/10.1016/j.scitotenv.2023.162196.

Welzel, M., Lange, A., Heider, D., Schwarz, M., Freisleben, B., Jensen, M., et al., 2020. Natrix: a Snakemake-based workflow for processing, clustering, and taxonomically assigning amplicon sequencing reads. BMC Bioinform. 21 (1), 526. https://doi.org/10.1186/s12859-020-03852-4.

Wickham, H., Averick, M., Bryan, J., Chang, W., McGowan, L., François, R., et al., 2019. Welcome to the Tidyverse. JOSS 4 (43), 1686. https://doi.org/10.21105/joss.01686.
Winking, C., Lorenz, A.W., Sures, B., Hering, D., 2014. Recolonisation patterns of benthic invertebrates: a field investigation of restored former sewage channels. Freshw. Biol. 59 (9), 1932–1944. https://doi.org/10.1111/fwb.12397.
Winking, C., Lorenz, A.W., Sures, B., Hering, D., 2016. Start at zero: succession of benthic invertebrate assemblages in restored former sewage channels. Aquat. Sci. 78 (4), 683–694. https://doi.org/10.1007/s00027-015-0459-7.